(12)

WSRL-0211-TR

AR-002-583

DEPARTMENT OF DEFENCE

DEFENCE SCIENCE AND TECHNOLOGY ORGANISATION

WEAPONS SYSTEMS RESEARCH LABORATORY

DEFENCE RESEARCH CENTRE SALISBURY
SOUTH AUSTRALIA

TECHNICAL REPORT

WSRL-0211-TR

THE USE OF A DEFLECTABLE NOSE ON A MISSILE AS A CONTROL DEVICE

K.D.THOMSON

Approved for Public Release

COPY No.

MAY 1981

AR-002-583

DEPARTMENT OF DEFENCE

DEFENCE SCIENCE AND TECHNOLOGY ORGANISATION

WEAPONS SYSTEMS RESEARCH LABORATORY

TECHNICAL REPORT

WSRL-0211-TR

THE USE OF A DEFLECTABLE NOSE ON A MISSILE AS A CONTROL DEVICE

K.D. Thomson

S U M M A R Y

Wind tunnel tests have been carried out on a blunted ogive-cylinder with a deflectable nose at Mach numbers between 0.8 and 2.0. Although the results are subject to scale effects, it appears that the deflectable nose could find use as a missile control method.

The results have been applied to two missile configurations. For a long slender missile the deflectable nose produces non-linear trim curves at subsonic speeds, approaching linearity at supersonic Mach numbers. Nevertheless, worthwhile trimmed incidences can be achieved. Although a deflectable nose on a 105 mm shell at subsonic speeds produces only relatively small normal force coefficients at trim, the trim curves are linear. Furthermore, it appears that when used for terminal control significant deviations in shell impact point are attainable.

POSTAL ADDRESS: Chief Superintendent, Weapons Systems Research Laboratory, Box 2151, GPO, Adelaide, South Australia, 5001.

TABLE OF CONTENTS

LIST OF FIGURES

1. INTRODUCTION

Most controllable missiles are steered by deflecting a set of control surfaces attached to the rear of the body. However, in recent years there has been a significant amount of research into the performance of canard control systems. This research has received impetus from the trend to extend the role and performance of existing missiles by the addition of modules; an example is the conversion of standard bombs into "smart" bombs. In such cases it is attractive, and simple in principle, to remove the front fuse and replace it by a target sensor, some rudimentary intelligence, and a control system to fly the missile towards a selected target. However, the protruding canard controls can cause a packaging problem in certain circumstances and, furthermore, their aerodynamic performance is not as good as might be expected; it might be thought that canards have an advantage over rear controls in that the lift force they generate in setting a statically stable missile at a trimmed incidence is in a direction to increase the missile's normal acceleration, whereas rear controls oppose the normal acceleration. However, if the missile carries lifting surfaces a few body diameters downstream of the canards, these surfaces tend to act as flow straighteners and remove the downwash imparted by the canard controls. In doing so they experience a decrease in normal force roughly equal to the canard control normal force. The net effect is that the canards provide a pitching moment and generally only a small contribution to the normal acceleration of the missile.

An alternative forward control for a missile might be a deflectable nose similar to the drooped nose of the Concorde aircraft, but being able to deflect in any plane. This would not affect the packaging characteristics of a missile, and because any nose lift due to nose deflection is accompanied by downwash generally in the lee of the body rather than spread laterally in the flow, downstream lifting surfaces may not be so effective in removing downwash. There is a possibility therefore that a deflectable nose may provide a suitable method of controlling a missile. Indeed, for a statically stable missile it could be imagined that a very simple missile steering method could be achieved by the nose always being pointed towards the target. The forces acting on the missile would then fly the missile towards the target.

Wind tunnel tests on the effectiveness of a deflectable nose on a typical missile body have been conducted to explore the concept. A slender ogive-cylinder with a rounded nose was chosen, and part of the curved nose was made deflectable. No lifting surfaces were attached to the model, the objective being to determine the control effectiveness of the deflectable nose in the absence of control or lifting surface interference. Force and moment measurements were made at both subsonic and supersonic speeds and sections of the results are included in this report. These results are then applied to estimate the controllability of two types of missile with deflectable noses, namely:

(a) a long slender missile with a rear stabilizer mounted so far aft that control/lifting surface interference should be negligible, and

(b) a 105 mm shell.

2. MODEL AND TEST PROCEDURE

The model (figure 1) is a 25 mm diameter(d) tangent ogive-cylinder having a 3d ogival nose shortened by spherical nose blunting, and a cylindrical afterbody of length 8d. The front portion was fitted with a spherical joint and an internal worm and wheel mechanism which enabled the front half of the nose to be

deflected in one plane through angles between 0° and 28°. A four component strain gauge balance was mounted within the body and measured normal and side forces, pitching and yawing moments. Base flow effects were negligible since the balance sting shroud was made a continuation of the model afterbody, but separated 1.5 mm from the rear of the model.

Wind tunnel measurements were conducted at Reynolds numbers based on diameter of 1.6 to 1.7 x 10^{5}. In order to force boundary layer transition, two rows of glass spheres were glued to the nose surface as shown in figure 1. Results of surface oil flow tests under conditions of subcritical cross-flow Mach number, (such as figure 2), indicate that the spheres were generally effective in producing a turbulent boundary layer; away from the nose region the boundary layer separates at an angular distance from the windward stagnation line of 105°, which is consistent with results for a circular cylinder with turbulent flow separation in the lower Reynolds number range of the supercritical region or in the transcritical range. However, the results must be subject to scale effects since under full scale flight conditions separation angles of from 105° to 115° would be expected, as indicated by the pressure distributions in figure 152 of reference 1 and in reference 2. For convenience the reference station for pitching and yawing moments was taken to be the nose-cylinder junction.

3. RESULTS

The wind tunnel test programme covered the following range of parameters:

Mach number M	Nose angle (degrees)	Pitch angle (degrees)	Roll angle (degrees)
0.80, 0.90, 0.95	0, 2, 4	0 to 25 in 1° steps	0 to 180 in 45° steps
0.80, 0.90, 0.95, 1.4, 2.0	8, 16, 25	0 to 30 in 1° steps	0 to 180 in 45° steps

A right-hand body axis system has been adopted to provide a sign convention for the forces and moments (figure 3). The nose was always deflected through a negative control angle ($\delta \leq 0^{\circ}$) at $\varphi = 0^{\circ}$ and the angles effectively became positive by rolling the model through 180°. For the $\varphi = 180^{\circ}$ cases the forces and moments have been reversed in sign in this report and the results are presented as if δ were altered in steps from -25° to $+25^{\circ}$. Results are presented in this report for $\varphi = 0^{\circ}$ and 180° only. The results for $\delta = 0^{\circ}$ are included in tabular form (Table 1 - these are plotted in figures 4 to 7). The aerodynamic characteristics for other values of δ can be found either from figures 4 to 7, or by the addition to $\delta = 0^{\circ}$ results of incremental forces and moments which are plotted in figures 8 and 9.

Force and moment coefficients (figures 4 to 7) are accurate to within 1% of full scale but in addition there is an absolute uncertainty in measurement which varies with Mach number and incidence, and is of a maximum order of 2% of local value for all coefficients. However, further errors could occur in the derivation of force and moment increments (figures 8 and 9) which were determined by graphical interpolation and differencing; the maximum error in $|\Delta C_{Z}|$ is believed to be 0.05 and in $|\Delta C_{m}|$ is 0.10. No experimental points have

been marked in figures 4 to 9 in order to minimise congestion.

4. DISCUSSION

4.1 Longitudinal Aerodynamic Characteristics

As is usual in tests on bodies of revolution, results on a given configuration at $\varphi = 0^{\circ}$ and $\varphi = 180^{\circ}$ are not identical. Examples illustrating the differences in normal force and pitching moment coefficients are shown for the $\delta = 0^{\circ}$ configuration in figures 4 and 5, by comparing the graphs marked " $\delta = 0^{\circ}$ " in the grouping for $\delta < 0^{\circ}$, with corresponding similarly marked graphs in the grouping for $\delta > 0^{\circ}$ (which, as stated in Section 3, really refer to results for $\varphi = 180^{\circ}$).

Figures 4 and 5 show quite clearly that, apart from at M = 2, negative nose angles (nose droop) cause very little change in the normal force coefficient, their main effect being to produce an increment in pitching moment. On the other hand, positive nose angles produce increments in both the normal force and pitching moment curves. These increments are shown plotted in figures 8 and 9. An ideal control is one which, for a fixed missile incidence, produces linearly varying normal force and pitching moment increments with change in control angle. Figures 8 and 9 show that the deflectable nose is far from ideal. However, if it is possible to keep away from combinations of incidence and control angle which are consistent with stalling of the control (for example, in figure 9(a) restricting the control angle below 15° for a body incidence of 25°), the controls exhibit orderly behaviour. In these circumstances it should be possible to design an effective control system based on a deflectable nose control concept. However, an examination of figures 4, 5, 8 and 9 does not indicate how effective such a control system would be. Accordingly, these results have been applied in an examination of the controllability of two types of missile. Discussion of the findings is deferred to Section 4.3.

4.2 Lateral Aerodynamic Characteristics

Again, changing roll angle from $\varphi = 0^{\circ}$ to $\varphi = 180^{\circ}$ for the $\delta = 0^{\circ}$ configuration is seen to have a significant effect on the aerodynamic properties. Differences in side force and yawing moment characteristics can be discerned by comparing corresponding columns in Table 1.

Numerous experiments (references 3 to 6 for example) have indicated that the development of side forces and yawing moments on a body of revolution at large angles of attack can be markedly affected by small changes in nose geometry. It might be expected therefore that deflecting the nose in the present experiments would dramatically alter the lateral aerodynamic characteristics. However, figures 6 and 7 show that at $\varphi = 0^{\circ}$ small control deflections produce only small changes to the side force and yawing moment coefficients and large deflections tend, if anything, to reduce them. A qualification to this comment is that at subsonic speeds the side forces and yawing moments are substantially increased at $\delta = +8^{\circ}$ for the incidence range 20 to 28°. Another surprising feature is an overall trend for C_Y to have a fairly consistent negative bias and C_n a positive bias for incidences less than about 20°; no dramatic changes develop as control angle is changed from nose-down to nose-up.

The relatively large magnitude of the maximum side force and yawing moment for $\delta = +8^{\circ}$ may be thought to constitute a problem area for a deflectable nose control system. However, for the two missile configurations examined in Section 4.3 a nose control deflection of $+8^{\circ}$ produces in each case a trimmed incidence much less than 20°. Therefore, if the missiles always fly near trimmed conditions, the circumstances for which large yawing moments and side forces occur should never be experienced. If they were experienced momentarily, it is possible that the missile could be rolled through an appropriate angle to counter the side forces and moments.

4.3 Application to Missile Configurations

As mentioned above, in order to judge whether the deflectable nose concept has any potential application for the missile designer, an assessment has been made of the controllability of two missile configurations with deflectable noses.

4.3.1 Long Slender Ogive-Cylinder ($\frac{L}{d} = 10.71$) Configuration with Stabilizer

The first configuration is based on the model in figure 1. The following assumptions have been made:

(a) The fins are so far from the nose that there is no significant interference between the nose and the stabilizer.

(b) The centre of gravity position is 5.5 diameters from the nose extremity.

(c) A rear stabilizer is attached such that it produces a linear normal force characteristic with incidence, the normal force acting one diameter ahead of the body base.

(d) The stabilizer size is such that at 5° incidence the missile static margin is 1 diameter for the whole Mach number range. In view of the fact that the stabilizer aerodynamic performance is affected by air compressibility, this assumption is tantamount to requiring a different size stabilizer on the configuration for each Mach number. The aerodynamic normal force characteristics must be calculated using the above condition, but it is not necessary to define the stabilizer shape physically.

By using figures 4, 5, 8 and 9 it is possible to calculate the trim curves, which are shown plotted in figure 10. The shape of the trim curves is not ideal in that they are highly non-linear in the transonic speed range; however, they approach linearity at supersonic speeds. Despite the non-linearity, for a maximum nose deflection of 25°, quite significant trimmed incidences of 10 to 20° can be achieved. It may be argued that in certain circumstances the non-linear trim curves could be a desirable feature, since they admit the possibility of a rather neat control system. When it is necessary to apply only a small lateral acceleration to the missile (control angle less than 20° say) the control behaves linearly, but when large lateral acceleration is required the control would be fully deflected and would perform as a bang-bang control system. Thus, in moderate manoeuvres there is the possibility of providing "fine tuning" of the lateral acceleration to satisfy missile requirements without the necessity for highly accurate angular setting of the controls.

It is noted that in the Mach number range 0.8 to 0.95 and with a fully deflected control, the trimmed attitude and normal force coefficient vary by a factor of more than 2. This sensitivity suggests that a missile with a deflectable nose may not be very accurate in the transonic range during high acceleration manoeuvres unless a sophisticated guidance system is employed.

4.3.2 105 mm Shell with Deflectable Nose Control

Jermey has carried out wind tunnel experiments on a 105 mm shell in its standard form(ref.7) and on a configuration in which the nose fuse was replaced by non-spinning cruciform canard controls(ref.8). A characteristic of a shell is that it is statically unstable and relies on a high spin rate to provide gyroscopic stability. Whereas a statically stable configuration requires the positive deflection of a forward control to generate a positive trimmed incidence (see for example the sketch inset in figure 10), a statically unstable configuration requires a negative control deflection (see sketch inset in figure 12). Thus, as Jermey (8) found, the 105 mm shell generated a lifting force by virtue of its incidence and an opposing contribution from the deflected canards. The net lateral force acting on the shell was very small and Jermey found that terminal control by use of canards was not really feasible. Under the conditions he imposed when terminal correction was applied to the shell (flying subsonically at that stage) the estimated maximum lateral deviation in impact point was 90 m.

Figures 4, 5, 8 and 9 show that at subsonic speeds the deflectable nose has the property of generating a pitching moment with very little normal force for negative deflection angles. Therefore, it appears that a 105 mm shell with a deflectable nose may generate larger lifting forces under trimmed flight conditions than the shell with canard controls. An assessment was therefore carried out at M = 0.8 and 0.9 on a 105 mm shell with two different size deflectable noses. It is assumed that the addition of the control and its equipment do not alter the centre of gravity position. Following Jermey (8) it is further assumed that the spin imparted to the shell (but not the nose which must be de-spun) maintains stability when the nose is deflected.

The two deflectable noses are shown in figure 11. In order to estimate the aerodynamic contribution due to nose deflection, it is necessary to choose an equivalent ogive-cylinder in each case. Thus, for deflectable nose 1 (figure 11(a)) the force and moment coefficient increments in figures 8 and 9 are applicable, but are based on a body with a diameter 0.81 d. Similarly, for deflectable nose 2 (figure 11(b)) the equivalent ogive-cylinder body diameter is 1.37 d.

Construction of the trim curves for deflectable nose 1 (figure 12(a)) is a straightforward application of Jermey's experimental data for the 105 mm shell(ref.7) and figures 8 and 9.

It is seen from figure 11(b) that the addition of the large deflectable nose 2 has been made possible by adding a parallel section of length 1.18 d to the main body, and this necessitates a modification to Jermey's data bank for the 105 mm shell(ref.7). By slender body theory the parallel portion of the shell does not generate a normal force; furthermore, the nose normal force gradient with incidence is -2 per radian, based on the body cross-sectional area. These two conditions are sufficient for the normal force and pitching moment data on the 105 mm shell to be modified to suit the elongated

configuration in figure 11(b). Thus, let Z_N, Z_T be the nose, tail normal forces acting at distances x_N, x_T from the centre of gravity, and let subscripts 1 and 2 refer respectively to the original and lengthened shell configurations.

The moments about the centre of gravity are given by:

$$M_{G1} = Z_N x_{N1} - Z_T x_T ,$$

$$M_{G2} = Z_N x_{N2} - Z_T x_T ,$$

where Z_N is known from slender body theory and M_{G1} has been measured in reference 7.

$$\therefore \quad M_{G2} = M_{G1} + Z_N (x_{N2} - x_{N1})$$

and $x_{N2} - x_{N1} = 1.18$ d.

According to slender body theory the normal force generated by the lengthened shell is the same as that generated by the original shell. Trim curves for the shell with deflectable nose 2 have been calculated and are shown in figure 12(b).

Bearing in mind the possible inaccuracy in figures 8 and 9, as already mentioned in Section 3, and the assumption in the derivation above, the trim curves in figure 12 should be regarded as providing indicative rather than definitive information. The trim curves appear to be linear, but trimmed normal force coefficients are very small. The maximum manoeuvring force coefficient achieved by Jermey (8) on the shell with canard control is 0.045 (made up of -0.03 for C_{Ztrim} and 0.03 for the maximum Magnus side force coefficient) and is provided as a bench mark in figures 12(a) and 12(b). By assuming the maximum Magnus side force coefficient to be the same as that obtained by Jermey (8) an estimate can be made of the maximum manoeuvring force coefficient for the shell with deflectable nose, as shown in the following table. Recalling that the shell with canard controls was estimated to deviate 90 m under terminal control, the deviation of a shell with a deflectable nose is estimated under the same conditions* to be as follows:

Control Configuration	Limiting Control angle (degrees)	Achieved C_{Ztrim}	Maximum manoeuvring force coefficient	Estimated deviation (m)
Deflectable Nose 1	-25^o	-0.025 to -0.030	0.039 to 0.042	75 to 85
Deflectable Nose 2	-25^o	-0.15 to -0.16	0.153 to 0.163	305 to 325
Canard Control (reference 8)	-30^o	-0.03	0,045	90

* Mean Mach number 0.75, shell spin rate 160 rev/s, manoeuvre phase lasting 16 s.

The smaller control (deflectable nose 1) is seen to be relatively ineffective, but deflectable nose 2 produces significant deviations in flight path. If the method of calculating the aerodynamic forces on the lengthened shell proves to be valid, and if the assumption is justified of maintaining gyroscopic stability, then the concept of using a deflectable nose for shell terminal correction appears to be worthy of further study. However, it should be borne in mind that the estimated deviation is critically dependent on the centre of gravity position, which has been assumed to be unchanged by the nose modification shown in figure 11(b). The expected forward cg movement would decrease the deviation and the figures in the above table must therefore be considered somewhat optimistic.

5. FINAL COMMENTS

The comments in this section are conditional upon the extent of scale effects in the wind tunnel test results.

It appears that a deflectable nose could be used in a control system for a missile, but it would not be ideal. Negative nose deflections produce a significant increment in pitching moment but small normal forces, while positive deflections produce significant increments in both pitching moment and normal force. Contrary to expectations, deflection of the nose did not have a dramatic effect on side force or yawing moment characteristics at zero roll angle.

Use of a deflectable nose to control a long slender statically stable missile configuration leads to highly non-linear trim curves at subsonic speeds, approaching linearity at supersonic speeds. Nevertheless, worthwhile trimmed incidences are achieved. A large deflectable nose control on a 105 mm shell at subsonic speeds provides linear trim curves. It appears that significant impact point deviations could be achieved when the nose is used to apply terminal control. This aspect is worthy of further study.

6. ACKNOWLEDGEMENT

The author is grateful to Mr J. Beniulis who designed the deflectable nose control mechanism in the wind tunnel model and to the tunnel operations team who carried out the wind tunnel experiments.

NOTATION

C_m	pitching moment coefficient = M/qSd
C_n	yawing moment coefficient = N/qSd
C_Y	side force coefficient = Y/qS
C_Z	normal force coefficient = Z/qS
C_{Ztrim}	normal force coefficient at trim
L	body length
M	pitching moment; also Mach number
M_G	pitching moment about CG position
N	yawing moment
S	reference area = $\pi\ d^2/4$
Y	side force
Z_N	nose normal force
Z_T	tail normal force
d	body diameter
q	dynamic pressure
x_N	distance from CG to point of action of nose normal force
x_T	distance from CG to point of action of tail normal force
α	angle of incidence
δ	nose deflection angle
θ	pitch angle
φ	roll angle

Subscripts 1, 2, refer respectively to standard and lengthened 105 mm shell

REFERENCES

No	Author	Title
1	Goldstein, S. (Editor)	"Modern Developments in Fluid Dynamics". Clarendon Press, 1950, pp 417 - 428
2	Roshko, A.	"Experiments on the flow past a circular cylinder at very high Reynolds number". Journal of Fluid Mechanics Vol 10, pp 345 - 356, 1961
3	Thomson, K.D. and Morrison, D.F.	"The spacing, position and strength of vortices in the wake of slender cylindrical bodies at large incidence". Journal of Fluid Mechanics, Vol 50, pp 751 - 783, 1971
4	Pick, G.S.	"Investigation of side forces on ogive cylinder bodies at high angles of attack in the $M = 0.5$ to 1.1 range". Journal of Spacecraft and Rockets, Vol 9, pp 389 - 390, June 1972
5	Lamont, P.J. and Hunt, B.L.	"Pressure and force distribution on a sharp-nosed circular cylinder at large angles of inclination to a uniform subsonic stream". Journal of Fluid Mechanics, Vol 76, pp 519 - 559, 1976
6	Almosnino, D. and Rom, J.	"Alleviation of the side force and yawing moment acting on a slender cone-cylinder body at high angles of attack, using small jet injection at subsonic and transonic speeds". Israel Institute of Technology, DAERO-78-G-119, 1979
7	Jermey, C.	"Wind tunnel tests on the static aerodynamics of a spinning 105 mm artillery shell model". Report WSRL-0090-TR, 1979
8	Jermey, C.	"Wind tunnel tests of a spinning 105 mm artillery shell model with canard control surfaces". Report WSRL-0122-TR, 1979

TABLE 1. AERODYNAMIC COEFFICIENTS FOR ZERO NOSE DEFLECTION ($\delta = 0^{o}$)

(a) $M = 0.80$, $\varphi = 0^{o}$

α (degrees)	C_Y	C_Z	C_m	C_n
-0.03	0.000	0.000	-0.005	0.010
0.98	-0.002	-0.037	0.038	0.014
2.00	-0.001	-0.075	0.070	0.015
3.02	-0.000	-0.117	0.082	0.012
4.03	0.000	-0.161	0.075	0.014
5.04	0.001	-0.214	0.025	0.011
6.06	0.000	-0.271	-0.048	0.009
7.07	0.000	-0.333	-0.145	0.008
8.08	-0.001	-0.401	-0.267	0.015
9.11	-0.001	-0.478	-0.418	0.019
10.12	-0.002	-0.556	-0.577	0.027
11.14	-0.003	-0.641	-0.757	0.028
12.16	-0.010	-0.730	-0.952	0.069
13.18	-0.016	-0.825	-1.165	0.104
14.19	-0.024	-0.918	-1.384	0.154
15.20	-0.031	-1.016	-1.625	0.197
16.22	-0.027	-1.123	-1.883	0.176
17.25	-0.037	-1.236	-2.161	0.237
18.27	-0.059	-1.356	-2.435	0.368
19.29	-0.067	-1.487	-2.713	0.418
20.32	-0.073	-1.621	-2.978	0.440
21.36	-0.061	-1.769	-3.275	0.374
22.33	-0.088	-1.905	-3.556	0.495
23.43	-0.164	-2.064	-3.875	0.831
24.45	-0.245	-2.220	-4.158	1.165
25.48	-0.306	-2.372	-4.400	1.334

TABLE 1(CONTD.).

(b) M = 0.80, φ = 180°

α (degrees)	C_Y	C_Z	C_m	C_n
0.03	-0.002	0.003	-0.001	0.008
-0.99	-0.001	0.040	-0.049	0.003
-2.00	-0.001	0.079	-0.081	0.003
-3.02	0.000	0.117	-0.113	-0.002
-4.02	-0.000	0.161	-0.110	0.000
-5.04	0.001	0.212	-0.072	-0.005
-6.06	0.000	0.269	-0.003	-0.008
-7.07	0.001	0.330	0.089	-0.006
-8.10	0.001	0.400	0.210	-0.009
-9.10	0.000	0.473	0.347	-0.009
-10.12	0.004	0.554	0.504	-0.026
-11.14	0.004	0.639	0.679	-0.030
-12.15	0.006	0.728	0.874	-0.040
-13.16	0.006	0.822	1.073	-0.055
-14.19	0.006	0.920	1.289	-0.048
-15.20	0.022	1.014	1.520	-0.144
-16.22	0.025	1.125	1.788	-0.167
-17.25	0.036	1.235	2.058	-0.231
-18.28	0.048	1.361	2.353	-0.301
-19.29	0.092	1.491	2.633	-0.555
-20.31	0.112	1.628	2.912	-0.663
-21.38	0.125	1.770	3.214	-0.713
-22.38	0.124	1.907	3.500	-0.698
-23.42	0.102	2.052	3.792	-0.580
-24.45	0.077	2.191	4.043	-0.431
-25.47	0.019	2.338	4.263	-0.155

TABLE 1(CONTD.).

(c) M = 0.90, φ = 0°

α (degrees)	C_Y	C_Z	C_m	C_n
-0.02	0.002	0.001	0.004	0.001
0.99	0.002	-0.034	0.062	0.002
2.00	0.001	-0.069	0.116	0.004
3.03	0.002	-0.110	0.138	0.005
4.02	0.001	-0.156	0.130	0.007
5.05	0.001	-0.205	0.100	0.009
6.07	0.002	-0.263	0.030	-0.001
7.07	0.002	-0.326	-0.064	0.003
8.09	0.002	-0.395	-0.188	0.002
9.11	-0.000	-0.469	-0.323	0.014
10.11	-0.001	-0.549	-0.480	0.014
11.15	-0.004	-0.637	-0.655	0.031
12.16	-0.006	-0.726	-0.837	0.048
13.18	-0.016	-0.813	-1.044	0.103
14.20	-0.020	-0.910	-1.258	0.137
15.22	-0.026	-1.014	-1.492	0.166
16.24	-0.036	-1.126	-1.745	0.224
17.26	-0.037	-1.251	-1.996	0.233
18.31	-0.039	-1.384	-2.261	0.247
19.33	-0.045	-1.529	-2.520	0.274
20.36	-0.066	-1.678	-2.805	0.388
21.40	-0.098	-1.831	-3.109	0.542
22.43	-0.156	-1.993	-3.433	0.808
23.47	-0.214	-2.153	-3.744	1.061
24.52	-0.187	-2.324	-4.024	0.861
25.56	-0.134	-2.518	-4.371	0.540

TABLE 1(CONTD.).

(d) M = 0.90, φ = 180°

α (degrees)	C_Y	C_Z	C_m	C_n
0.04	-0.002	0.003	-0.001	0.007
-1.00	-0.001	0.039	-0.056	0.007
-2.00	-0.002	0.074	-0.115	0.005
-3.03	0.000	0.113	-0.160	-0.003
-4.03	-0.000	0.158	-0.168	0.003
-5.04	0.001	0.207	-0.133	-0.007
-6.07	0.001	0.265	-0.073	-0.005
-7.08	0.002	0.328	0.013	-0.008
-8.10	0.001	0.394	0.129	-0.004
-9.11	0.001	0.470	0.268	-0.012
-10.12	0.002	0.552	0.423	-0.017
-11.17	0.003	0.638	0.594	-0.018
-12.17	0.001	0.727	0.777	-0.017
-13.19	0.003	0.817	0.973	-0.026
-14.21	0.009	0.917	1.185	-0.059
-15.22	0.020	1.015	1.409	-0.131
-16.25	0.022	1.128	1.662	-0.138
-17.27	0.024	1.251	1.920	-0.160
-18.32	0.037	1.385	2.177	-0.232
-19.33	0.066	1.521	2.436	-0.399
-20.37	0.062	1.684	2.731	-0.366
-21.40	0.032	1.836	3.044	-0.202
-22.44	-0.020	2.003	3.354	0.058
-23.51	-0.062	2.175	3.672	0.222
-24.54	-0.050	2.345	3.966	0.146
-25.58	-0.015	2.534	4.333	-0.035

TABLE 1(CONTD.).

(e) M = 0.95, φ = 0°

α (degrees)	C_Y	C_Z	C_m	C_n
-0.01	0.001	0.002	0.011	0.004
1.00	0.001	-0.033	0.080	0.005
2.00	0.001	-0.068	0.133	0.006
3.04	0.000	-0.108	0.171	0.011
4.04	0.001	-0.151	0.179	0.009
5.04	0.002	-0.201	0.152	0.004
6.07	0.002	-0.259	0.083	0.003
7.09	0.002	-0.321	-0.006	0.002
8.14	0.002	-0.392	-0.125	0.003
9.13	0.000	-0.466	-0.246	0.010
10.14	-0.002	-0.548	-0.402	0.022
11.16	-0.005	-0.632	-0.563	0.039
12.17	-0.008	-0.718	-0.740	0.063
13.19	-0.017	-0.811	-0.936	0.116
14.22	-0.022	-0.914	-1.143	0.150
15.24	-0.027	-1.019	-1.372	0.171
16.26	-0.038	-1.135	-1.612	0.234
17.30	-0.029	-1.266	-1.858	0.182
18.35	-0.024	-1.404	-2.110	0.161
19.36	-0.023	-1.548	-2.373	0.150
20.39	-0.044	-1.695	-2.644	0.270
21.45	-0.043	-1.878	-2.950	0.259
22.49	-0.095	-2.055	-3.281	0.492
23.55	-0.113	-2.247	-3.620	0.552
24.59	-0.088	-2.441	-3.958	0.423
25.63	-0.054	-2.667	-4.406	0.219

TABLE 1(CONTD.).

(f) M = 0.95, φ = 180°

α (degrees)	C_Y	C_Z	C_m	C_n
0.03	-0.001	0.003	0.002	0.008
-0.99	-0.001	0.037	-0.074	0.007
-2.01	-0.000	0.072	-0.143	0.002
-3.06	0.002	0.112	-0.189	-0.006
-4.04	-0.000	0.153	-0.204	-0.001
-5.05	0.001	0.201	-0.180	-0.002
-6.08	0.001	0.259	-0.131	-0.005
-7.09	0.000	0.321	-0.037	-0.001
-8.11	0.001	0.392	0.066	-0.009
-9.12	0.002	0.465	0.196	-0.017
-10.14	0.002	0.550	0.345	-0.014
-11.17	0.000	0.635	0.500	-0.001
-12.18	-0.002	0.719	0.693	0.005
-13.20	0.000	0.815	0.880	-0.009
-14.22	0.002	0.914	1.079	-0.020
-15.24	0.021	1.018	1.303	-0.122
-16.27	0.017	1.141	1.533	-0.114
-17.30	0.012	1.266	1.778	-0.079
-18.34	0.046	1.406	2.020	-0.265
-19.36	0.048	1.550	2.279	-0.270
-20.40	0.075	1.715	2.557	-0.406
-21.45	0.086	1.876	2.884	-0.451
-22.50	0.030	2.046	3.194	-0.168
-23.54	0.023	2.224	3.540	-0.165
-24.59	0.039	2.451	3.913	-0.214
-25.63	0.048	2.674	4.372	-0.221

TABLE 1(CONTD.).

(g) M = 1.40, φ = 0°

α (degrees)	C_Y	C_Z	C_m	C_n
-0.02	-0.000	0.002	0.023	0.003
1.01	-0.000	-0.039	0.088	0.002
2.04	-0.000	-0.083	0.138	0.001
3.06	-0.001	-0.130	0.173	0.003
4.08	-0.000	-0.183	0.171	0.000
5.08	-0.001	-0.241	0.138	0.004
6.12	-0.001	-0.309	0.059	0.005
7.14	-0.000	-0.386	-0.058	0.001
8.16	-0.000	-0.471	-0.198	0.000
9.20	-0.001	-0.565	-0.365	0,010
10.21	-0.001	-0.664	-0.542	0.005
11.25	-0.002	-0.777	-0.754	0.014
12.28	-0.007	-0.900	-0.981	0.039
13.32	0.004	-1.035	-1.236	-0.023
14.36	0.003	-1.194	-1.565	-0.013
15.40	-0.001	-1.381	-1.945	0.010
16.45	-0.008	-1.595	-2.402	0.048
17.52	-0.020	-1.826	-2.936	0.109
18.59	-0.027	-2.087	-3.586	0.148
19.63	-0.030	-2.368	-4.315	0.156
20.70	-0.040	-2.678	-5.133	0.219
21.79	-0.051	-3.019	-6.036	0.275
22.86	-0.041	-3.369	-6.983	0.224
23.95	-0.004	-3.723	-7.962	0.048
25.01	-0.036	-4.082	-8.948	0.187
26.08	-0.058	-4.439	-9.951	0.294
27.17	-0.078	-4.811	-11.031	0.375
28.23	-0.027	-5.175	-12.143	0.138
29.29	-0.059	-5.549	-13.330	0.267
30.36	-0.087	-5.929	-14.578	0.349

TABLE 1(CONTD.).

(h) M = 1.40, φ = 180°

α (degrees)	C_Y	C_Z	C_m	C_n
0.01	-0.001	0.007	-0.001	0.010
-1.00	-0.002	0.048	-0.064	0.010
-2.03	-0.002	0.092	-0.113	0.008
-3.06	-0.001	0.140	-0.146	0.005
-4.07	-0.001	0.192	-0.153	0.002
-5.09	-0.003	0.252	-0.122	0.011
-6.12	-0.003	0.320	-0.047	0.013
-7.15	-0.003	0.399	0.073	0.015
-8.17	-0.003	0.485	0.221	0.012
-9.20	-0.002	0.581	0.393	0.005
-10.22	-0.001	0.682	0.572	-0.002
-11.25	-0.001	0.794	0.777	-0.002
-12.30	0.001	0.917	1.001	-0.012
-13.33	-0.004	1.055	1.252	0.019
-14.37	-0.002	1.217	1.568	0.016
-15.41	0.023	1.401	1.976	-0.120
-16.45	0.033	1.618	2.455	-0.184
-17.53	0.023	1.869	3.041	-0.115
-18.60	0.059	2.163	3.820	-0.319
-19.65	0.027	2.433	4.519	-0.159
-20.72	0.036	2.762	5.405	-0.188
-21.80	0.095	3.119	6.425	-0.522
-22.88	0.157	3.476	7.435	-0.884
-23.96	0.080	3.834	8.424	-0.463
-25.03	0.185	4.205	9.530	-0.978
-26.10	0.182	4.571	10.573	-0.948
-27.19	0.057	4.916	11.500	-0.319
-28.23	0.151	5.269	12.556	-0.747
-29.30	0.124	5.635	13.696	-0.617
-30.38	0.086	6.010	14.882	-0.438

TABLE 1(CONTD.).

(i) M = 2.00, φ = 0°

α (degrees)	C_Y	C_Z	C_m	C_n
-0.01	-0.011	0.003	0.042	0.079
1.00	-0.003	-0.047	0.057	0.010
2.03	-0.003	-0.097	0.097	0.013
3.07	-0.002	-0.152	0.118	0.003
4.07	-0.003	-0.210	0.113	0.007
5.11	-0.003	-0.281	0.072	0.009
6.13	-0.002	-0.360	-0.010	0.005
7.17	-0.003	-0.453	-0.136	0.013
8.20	-0.006	-0.555	-0.295	0.034
9.23	-0.008	-0.672	-0.490	0.047
10.28	-0.008	-0.817	-0.798	0.049
11.30	-0.003	-0.991	-1.239	0.015
12.34	-0.003	-1.190	-1.724	0.012
13.42	0.003	-1.418	-2.294	-0.026
14.44	0.001	-1.657	-2.910	-0.015
15.50	0.004	-1.910	-3.609	-0.035
16.56	-0.000	-2.169	-4.347	-0.013
17.61	-0.002	-2.440	-5.141	0.001
18.67	-0.006	-2.717	-5.984	0.017
19.71	-0.010	-2.993	-6.840	0.037
20.78	-0.013	-3.278	-7.724	0.058
21.83	-0.014	-3.563	-8.610	0.063
22.90	-0.019	-3.853	-9.524	0.080
23.95	-0.020	-4.140	-10.430	0.088
24.99	-0.010	-4.428	-11.352	0.044
26.05	-0.005	-4.727	-12.331	0.029
27.11	-0.004	-5.029	-13.328	0.026
28.14	-0.008	-5.333	-14.345	0.045
29.21	-0.005	-5.647	-15.400	-0.009
30.24	-0.005	-5.950	-16.421	-0.010

TABLE 1(CONTD.).

(j) M = 2.00, φ = 180°

α (degrees)	C_Y	C_Z	C_m	C_n
0.01	-0.007	0.001	-0.092	0.047
-1.02	-0.001	0.061	-0.035	0.001
-2.03	-0.001	0.110	-0.079	0.004
-3.06	-0.002	0.166	-0.096	0.004
-4.07	-0.001	0.228	-0.080	-0.004
-5.10	-0.001	0.298	-0.029	-0.006
-6.14	-0.001	0.380	0.062	-0.005
-7.16	0.001	0.474	0.200	-0.015
-8.21	0.006	0.584	0.380	-0.043
-9.23	0.004	0.709	0.642	-0.040
-10.25	0.007	0.867	1.027	-0.045
-11.32	0.002	1.060	1.561	-0.016
-12.34	0.007	1.288	2.256	-0.041
-13.40	0.009	1.526	2.900	-0.051
-14.45	0.017	1.762	3.494	-0.097
-15.49	0.016	2.004	4.124	-0.088
-16.56	0.016	2.258	4.815	-0.088
-17.61	0.012	2.514	5.529	-0.064
-18.68	0.015	2.785	6.322	-0.076
-19.72	0.019	3.053	7.129	-0.095
-20.77	0.026	3.331	7.982	-0.130
-21.83	0.032	3.619	8.872	-0.156
-22.88	0.035	3.902	9.759	-0.169
-23.96	0.044	4.200	10.704	-0.204
-25.00	0.035	4.493	11.652	-0.141
-26.07	0.028	4.795	12.631	-0.079
-27.12	0.020	5.099	13.628	-0.028
-28.15	0.012	5.401	14.636	0.014
-29.20	0.002	5.714	15.694	0.074
-30.26	-0.001	6.016	16.715	0.077

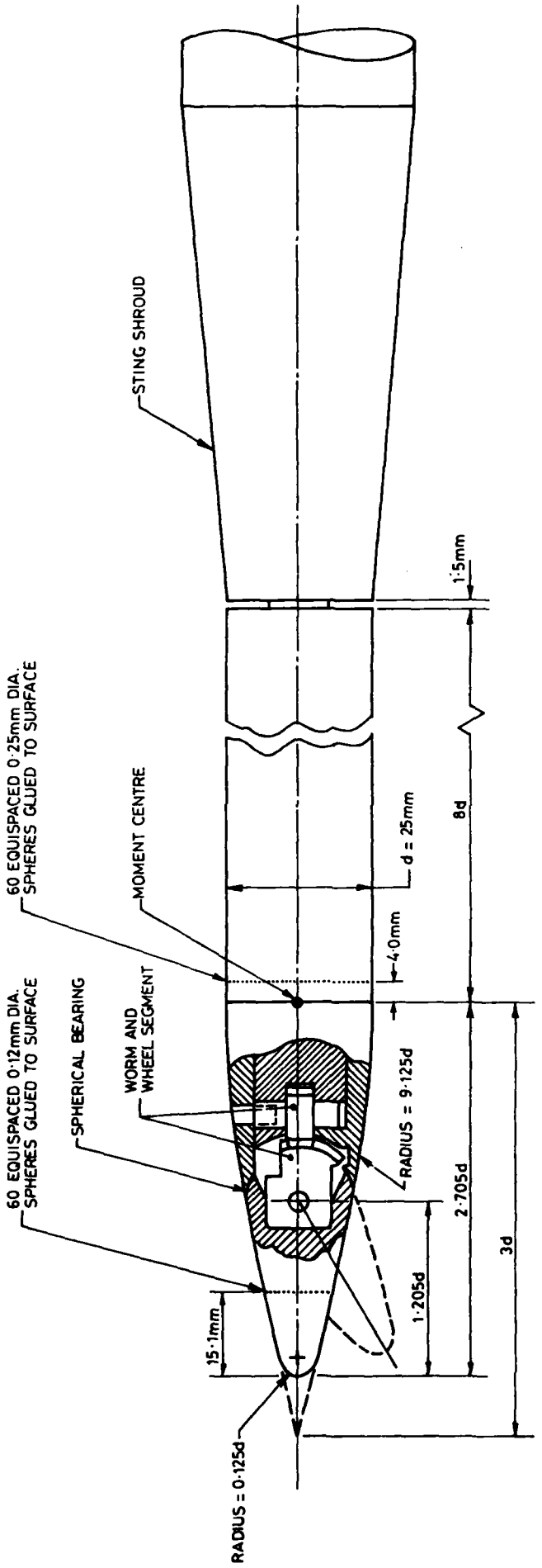

Figure 1. Ogive-cylinder with deflectable nose - details of wind tunnel model

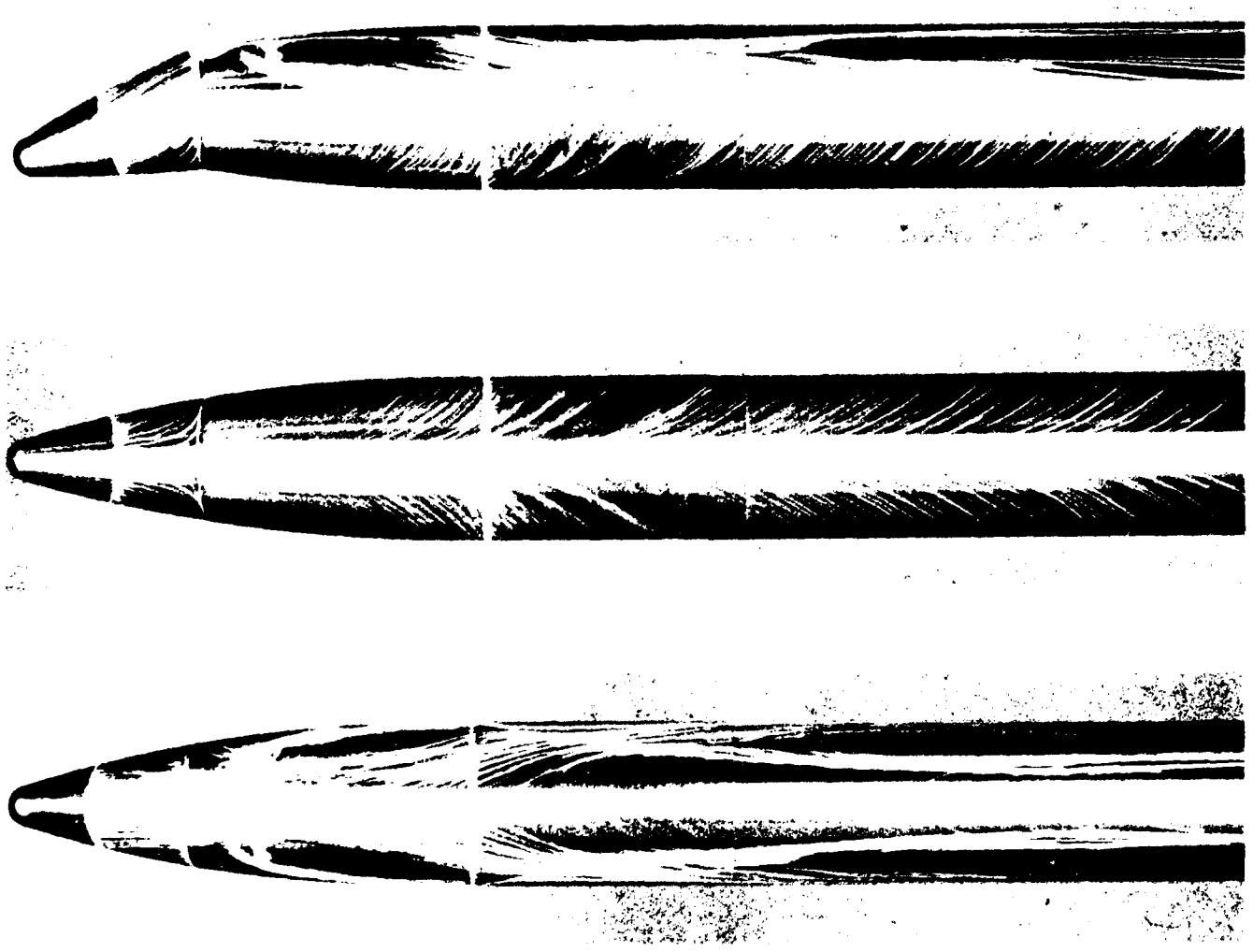

(a) Side view

(b) View from below

(c) View from above

Figure 2. Surface oil flow pattern for nose deflection - 16^{o}, incidence 21^{o}, Mach no. 0.9

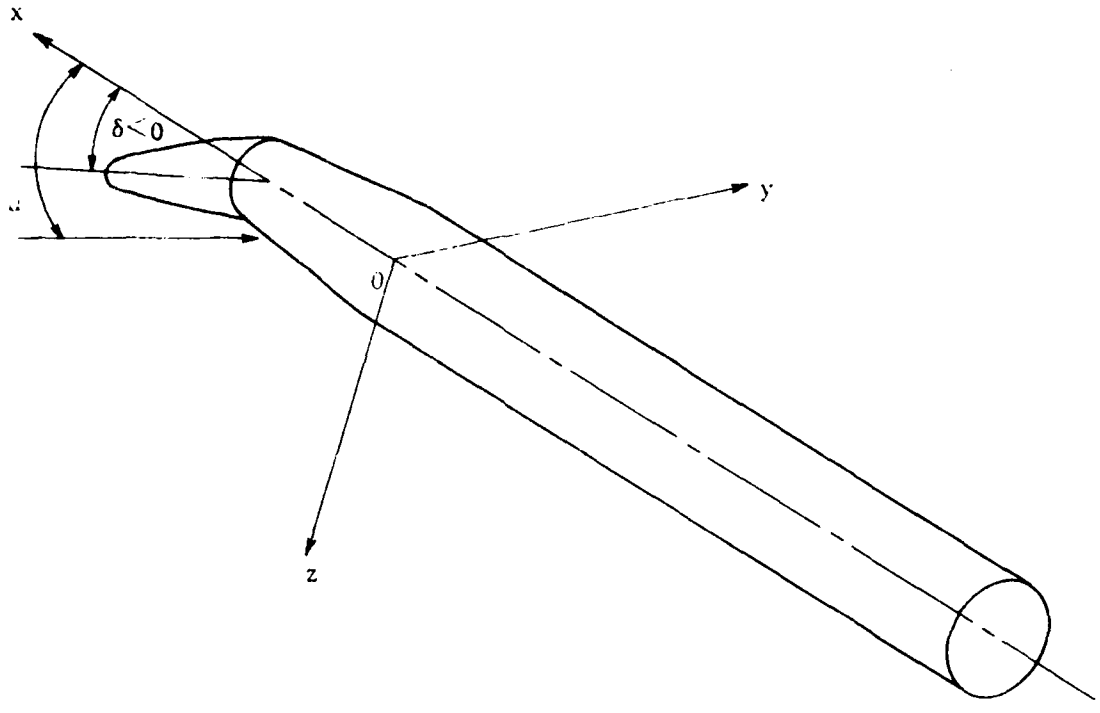

Figure 3. Body axis system used for defining sign of forces and moments

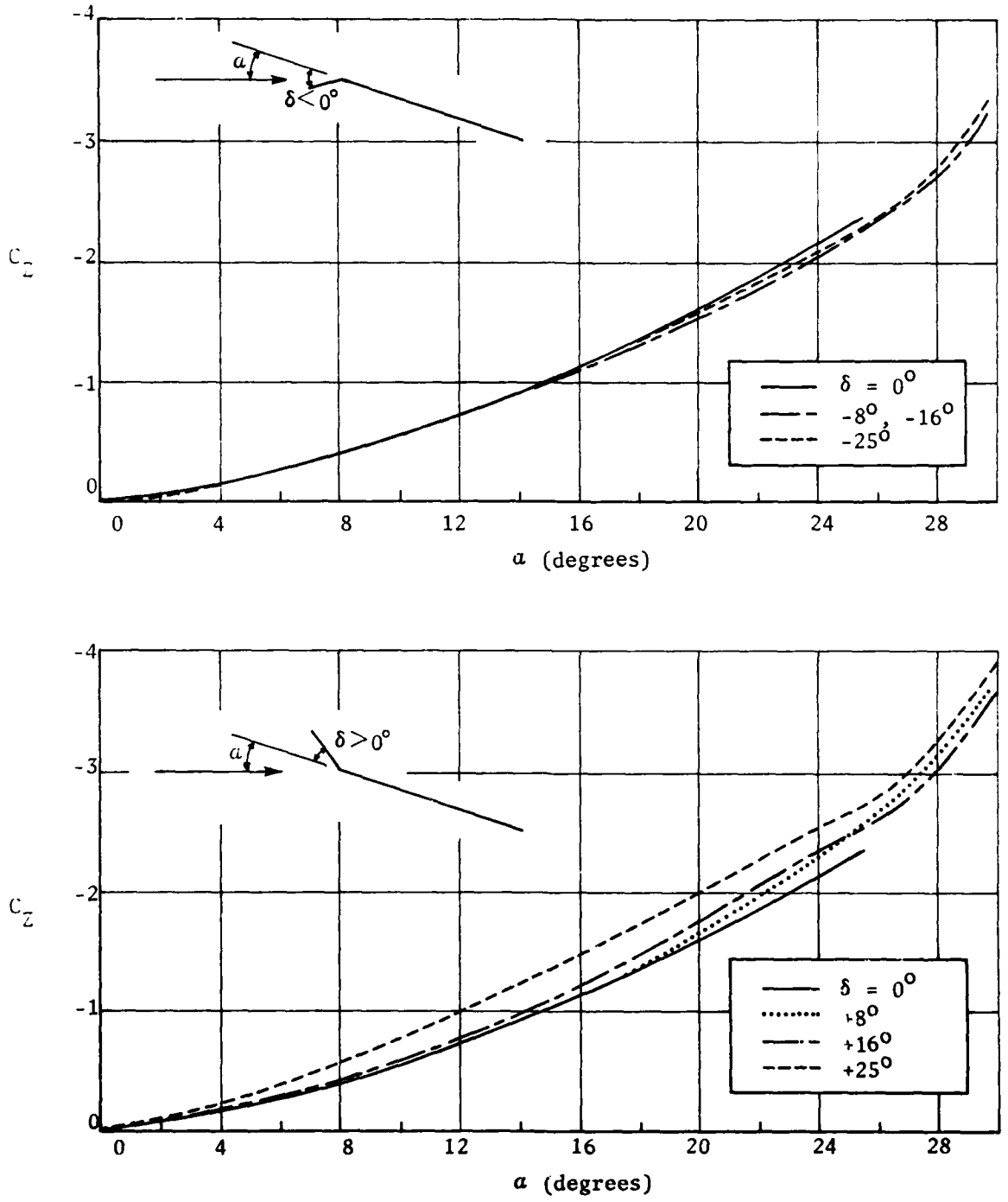

Figure 4(a). Normal force characteristics
M = 0.80

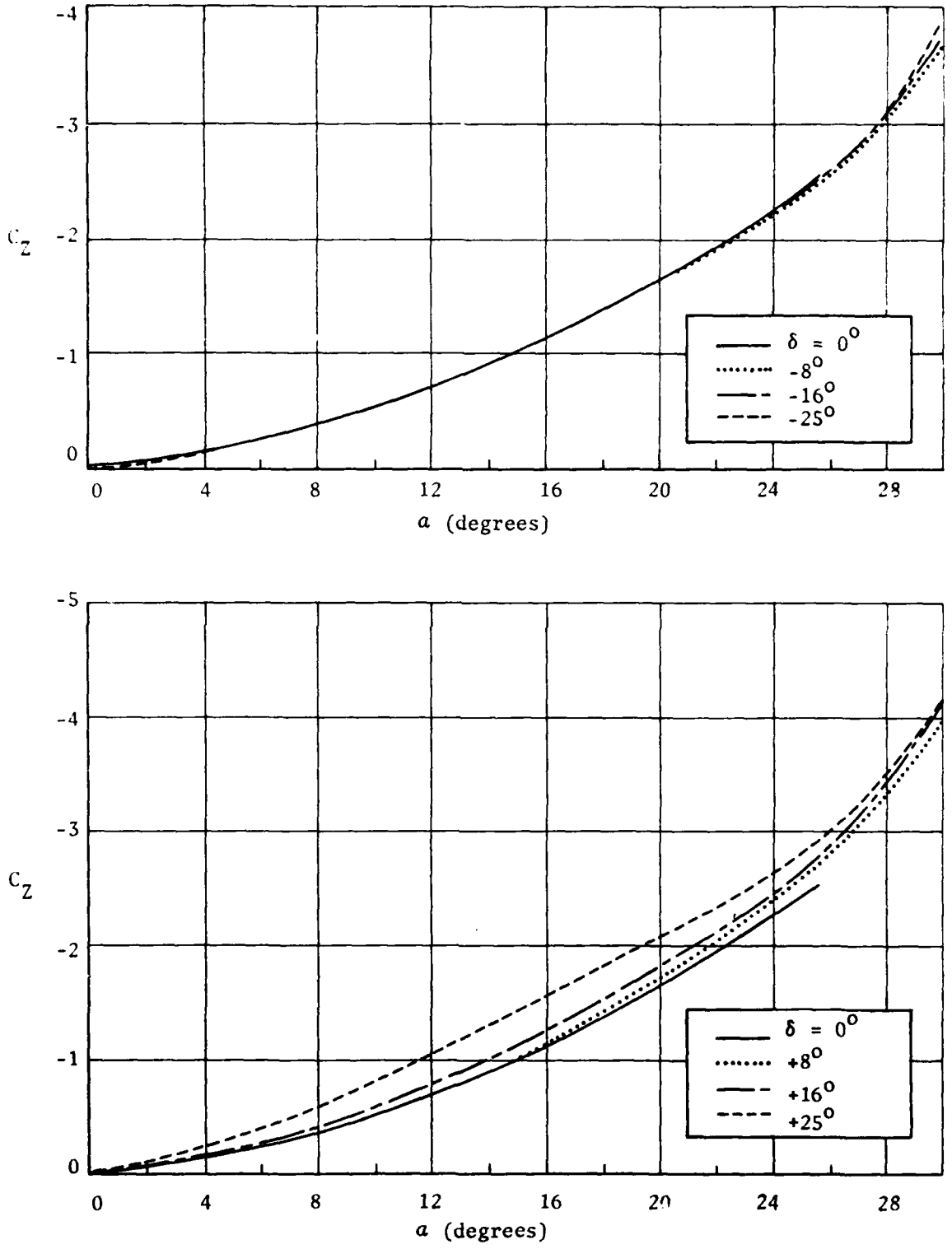

Figure 4(b). Normal force characteristics
M = 0.90

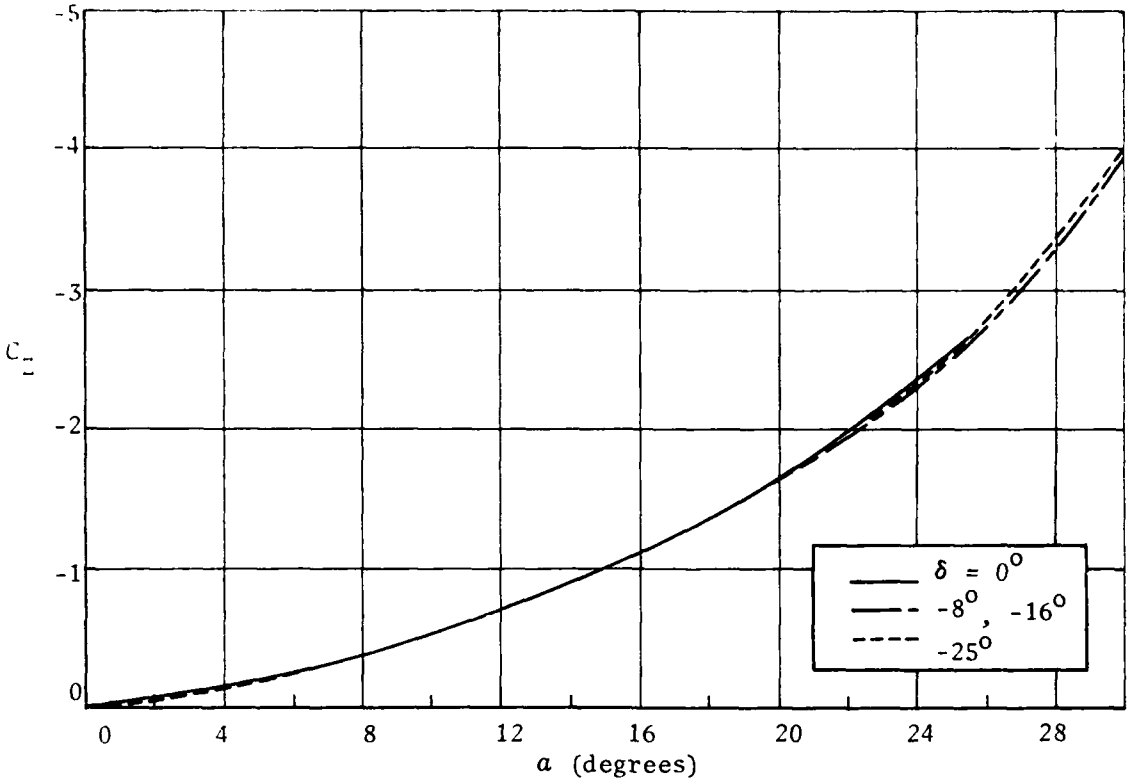

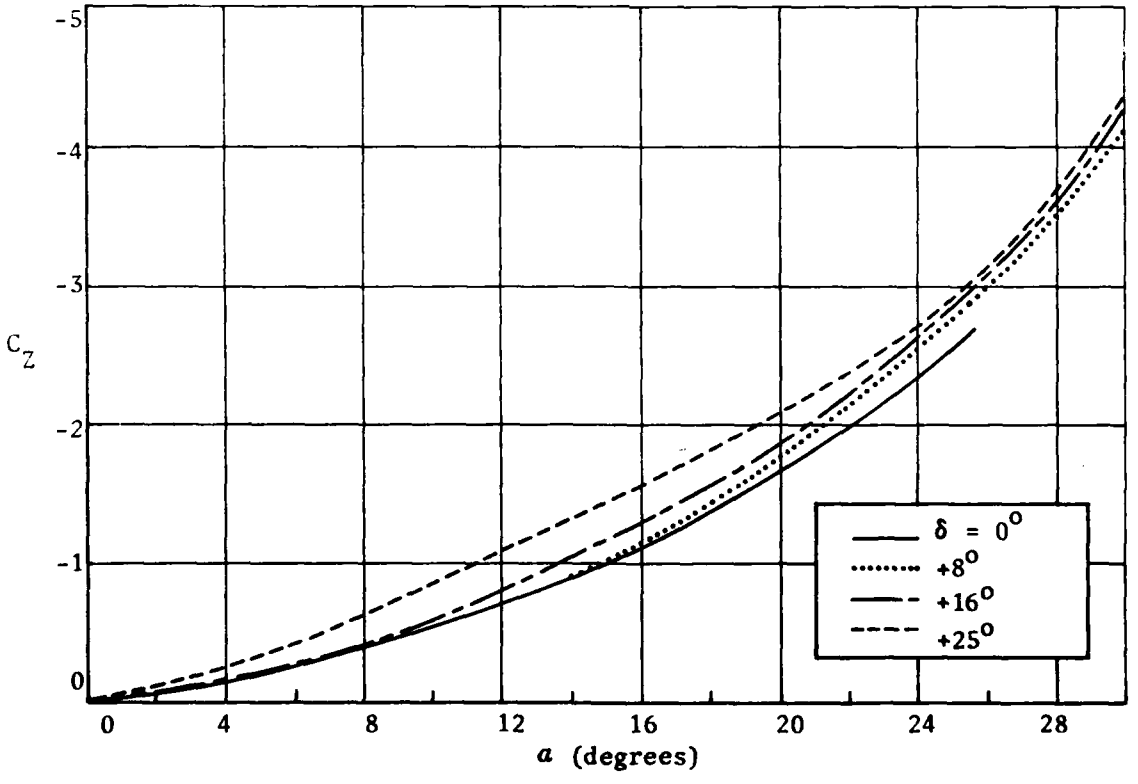

Figure 4(c). Normal force characteristics
M = 0.95

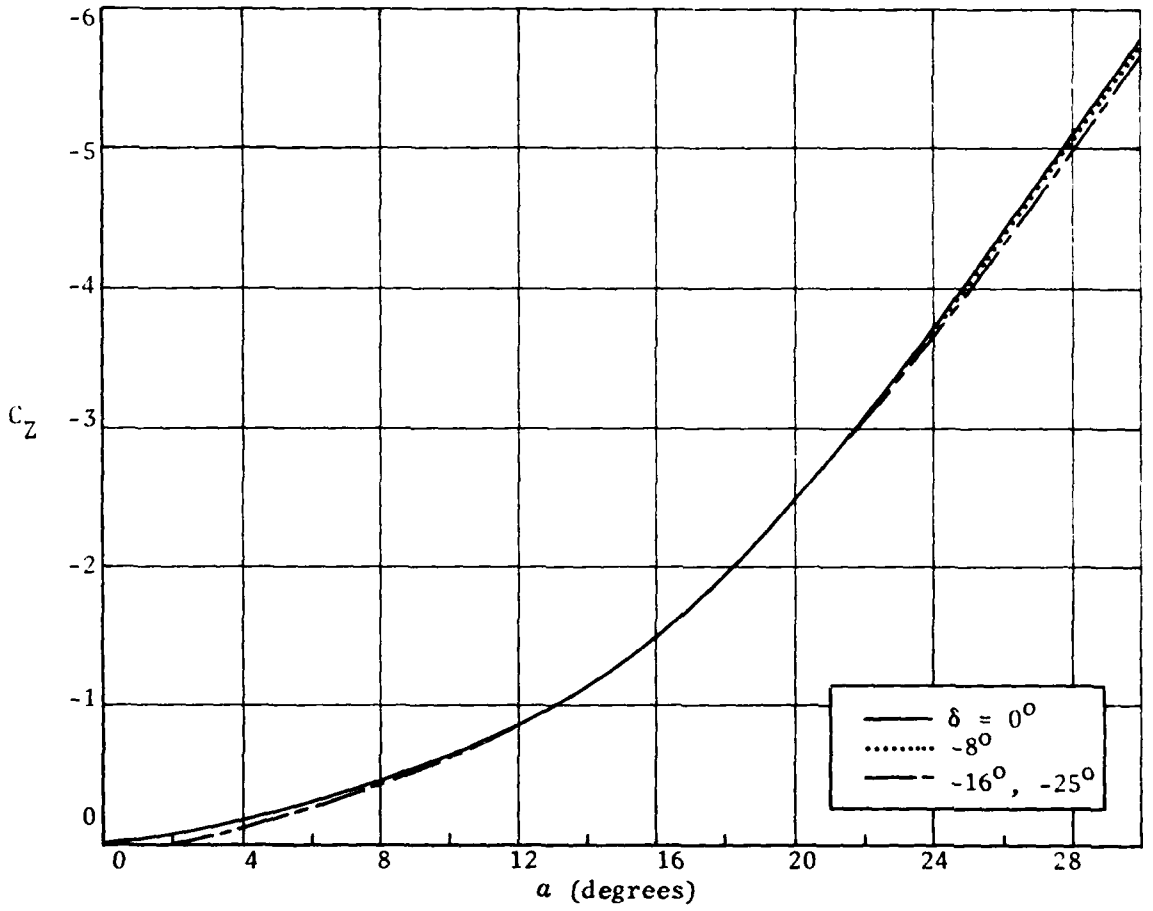

Figure 4(d). Normal force characteristics
M = 1.40

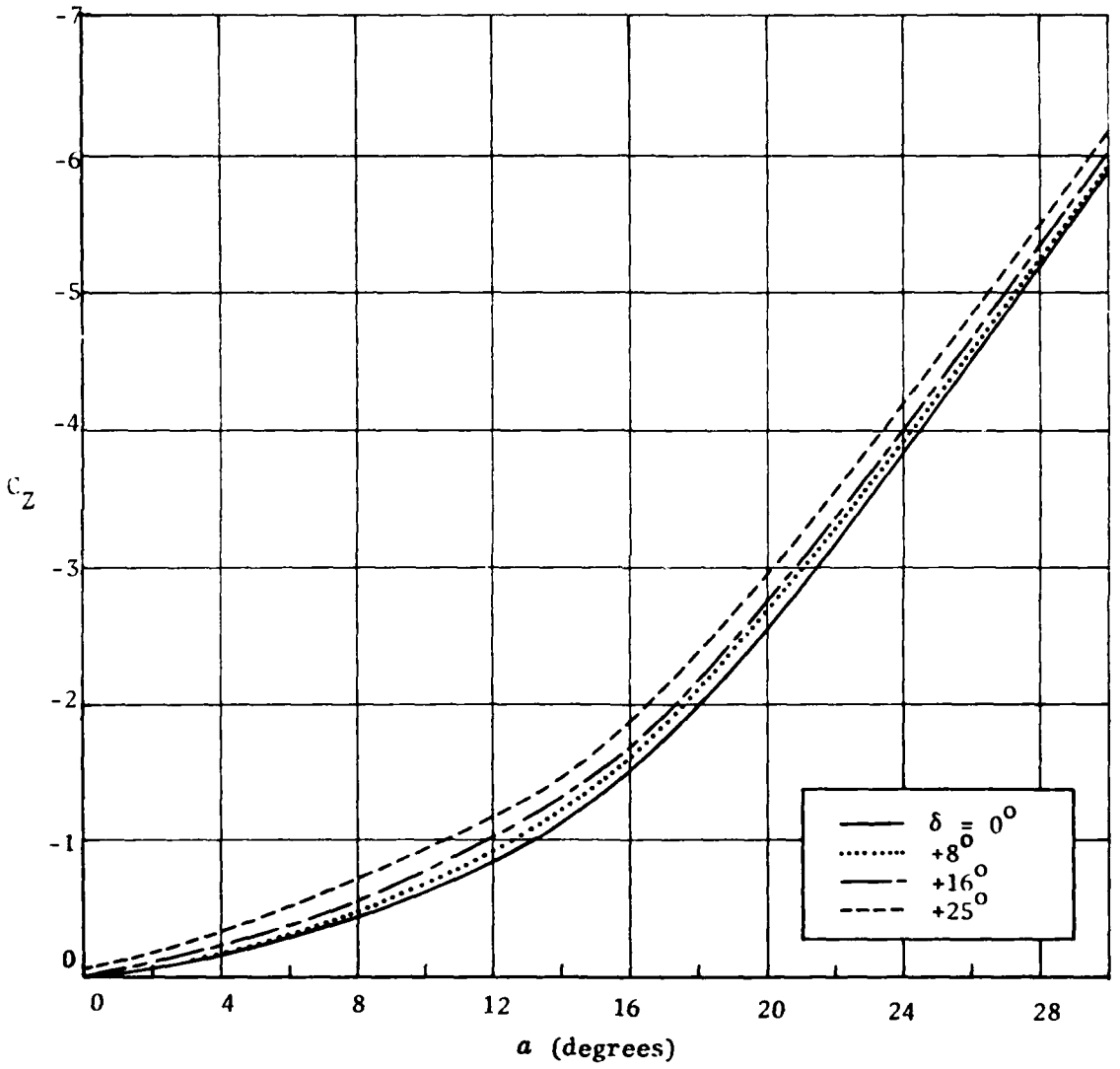

Figure 4(d)(Contd.).

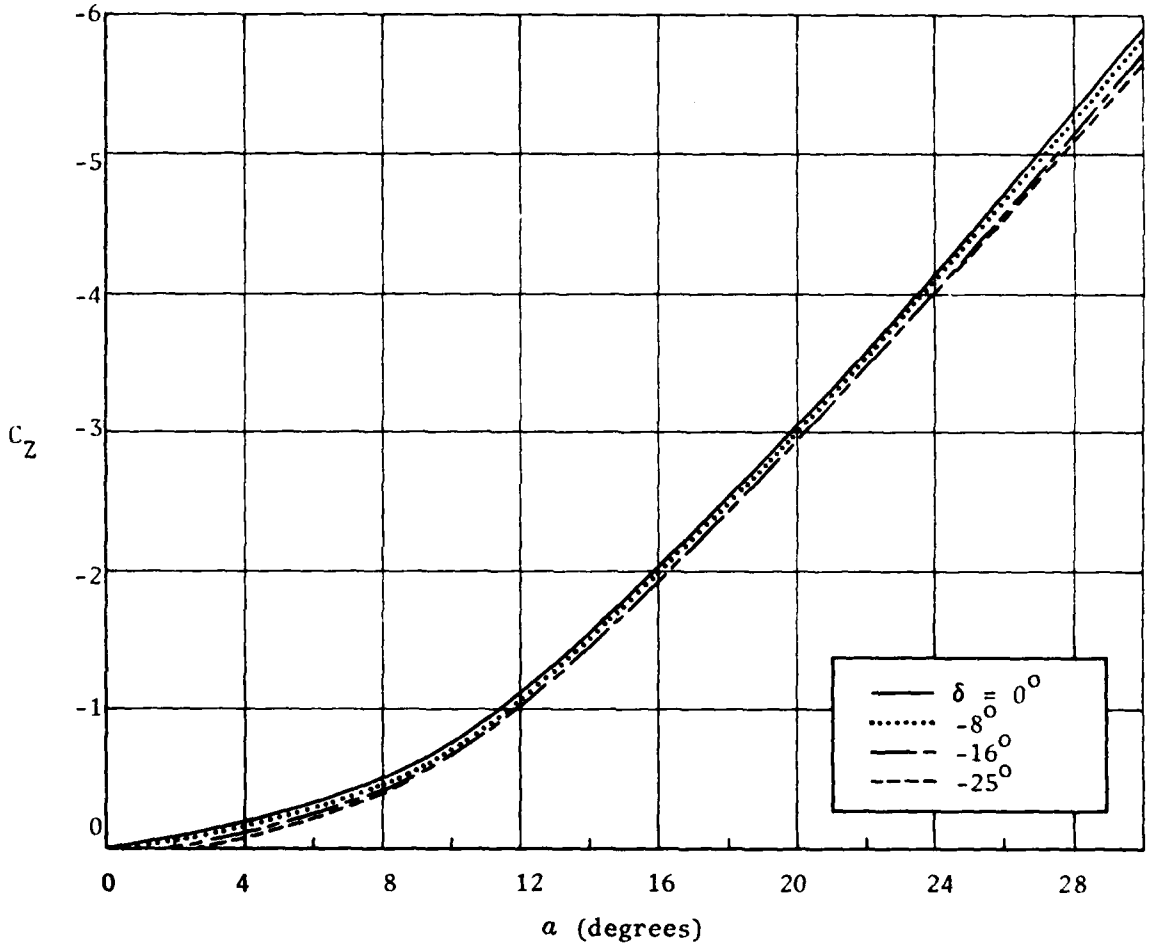

Figure 4(e). Normal force characteristics
M = 2.00

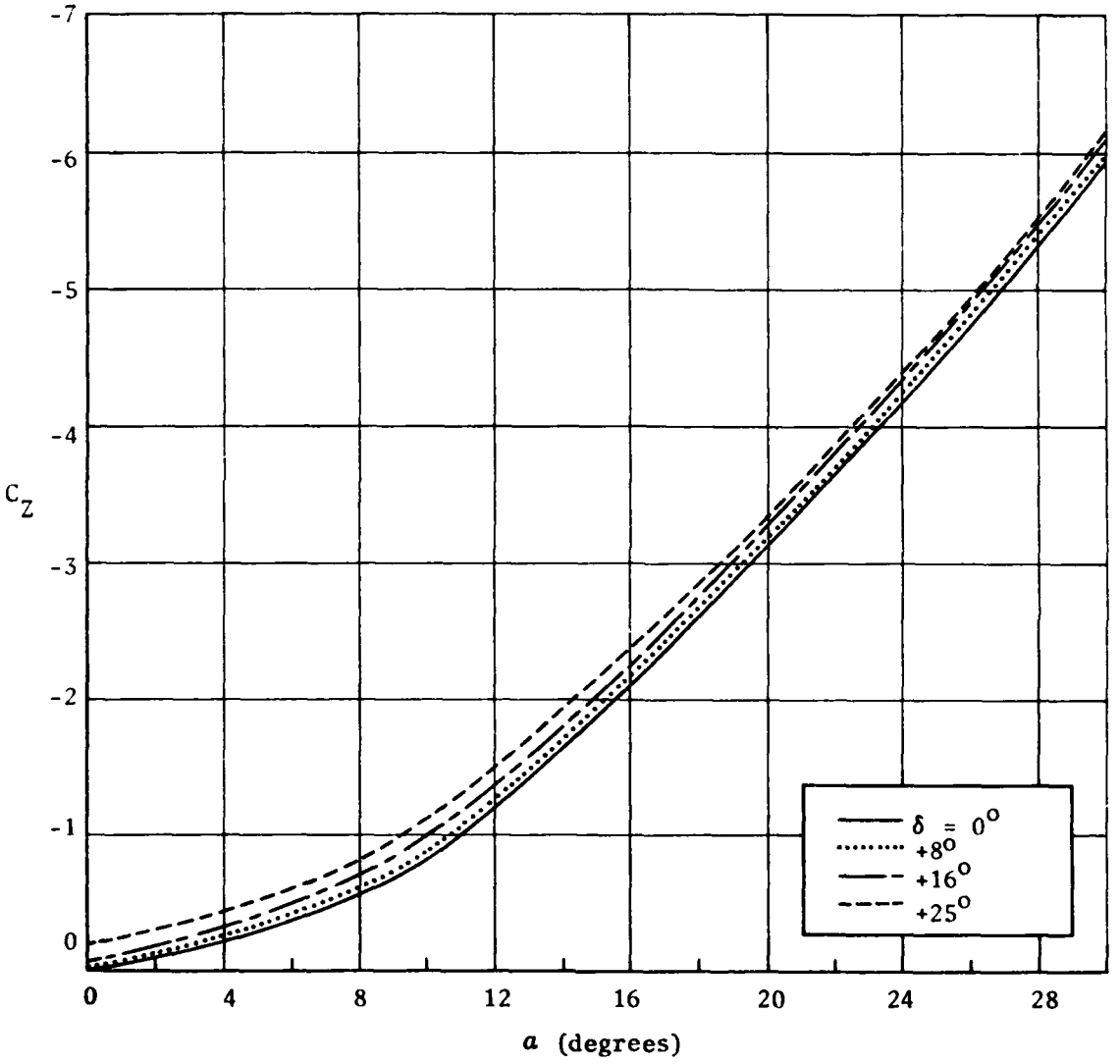

Figure 4(e)(Contd.).

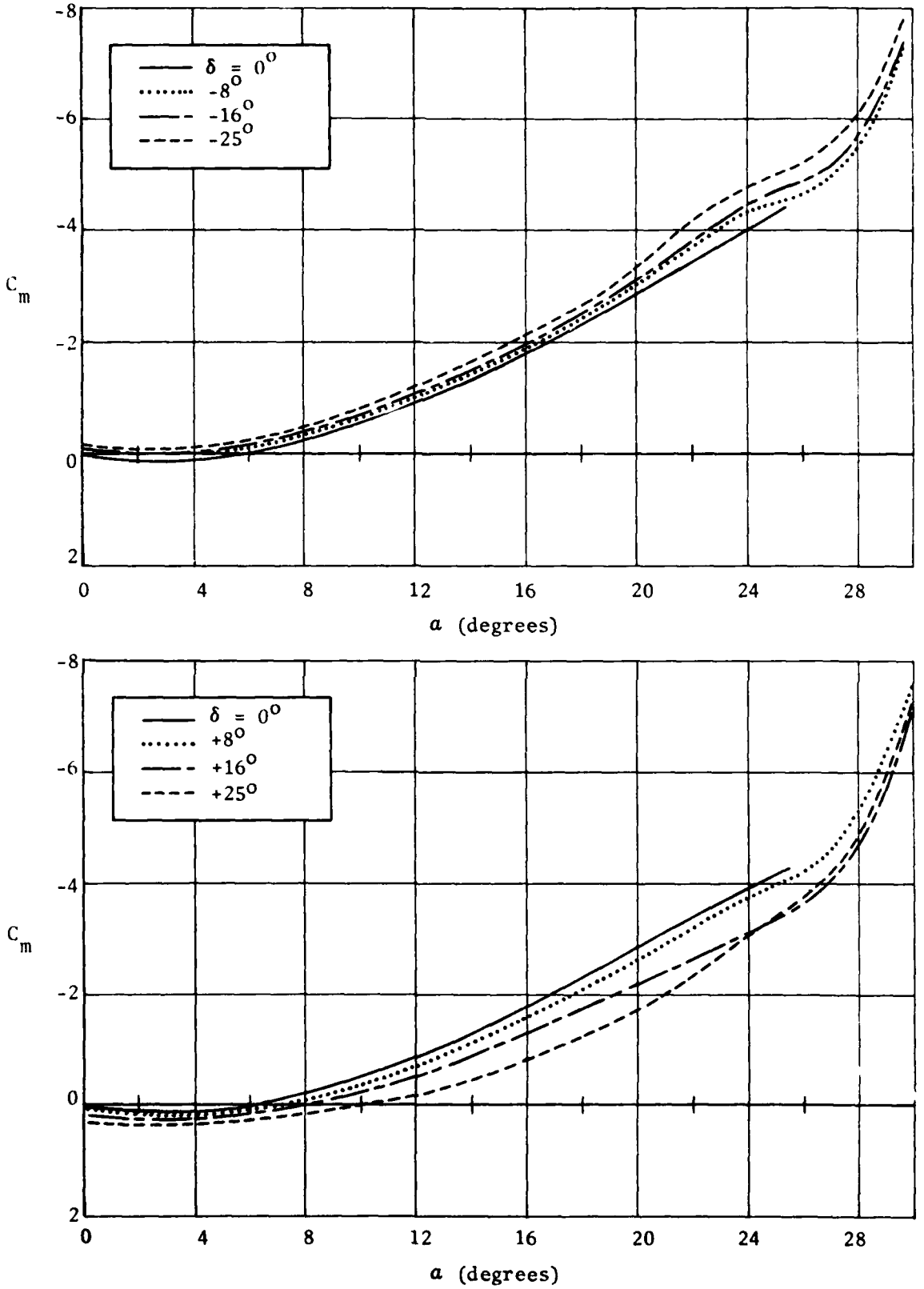

Figure 5(a). Pitching moment characteristics
M = 0.80

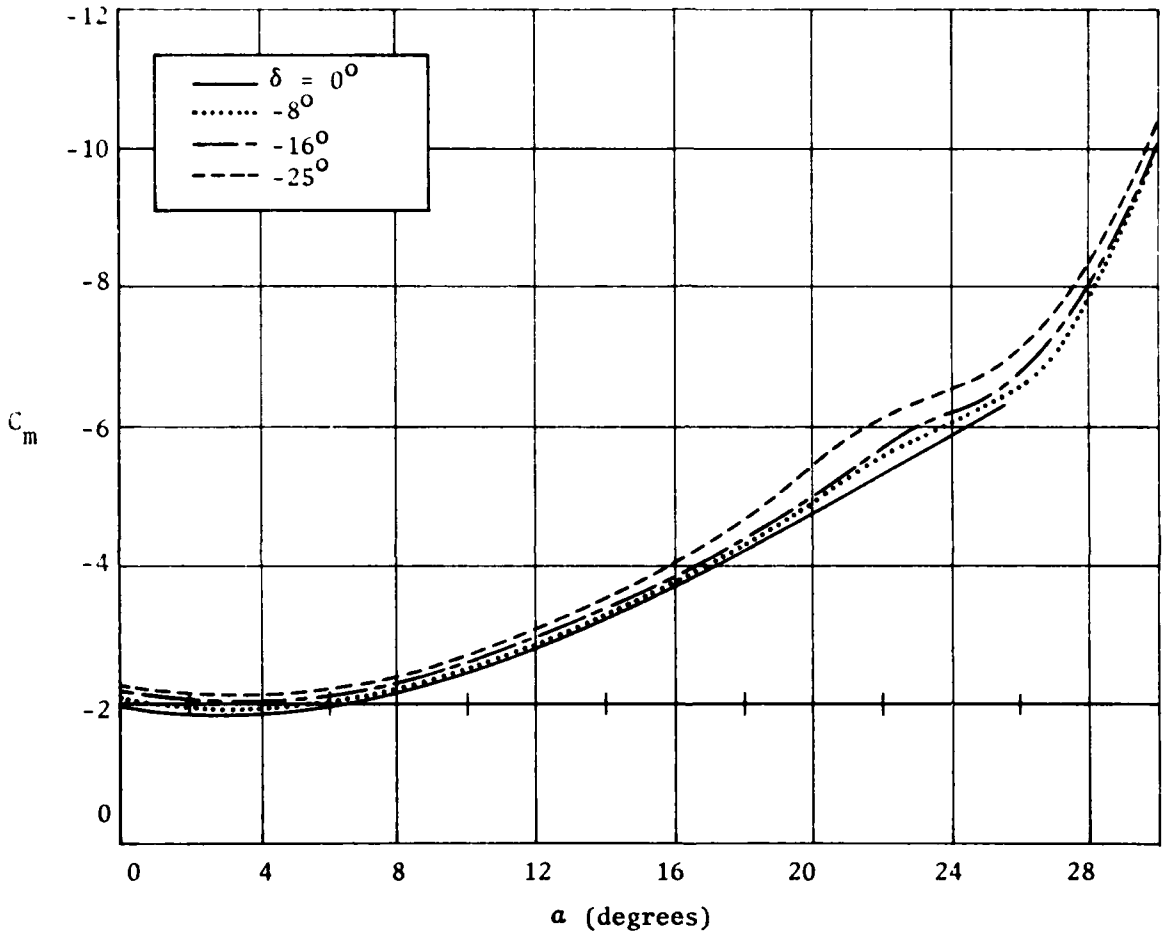

Figure 5(b). Pitching moment characteristics
M = 0.90

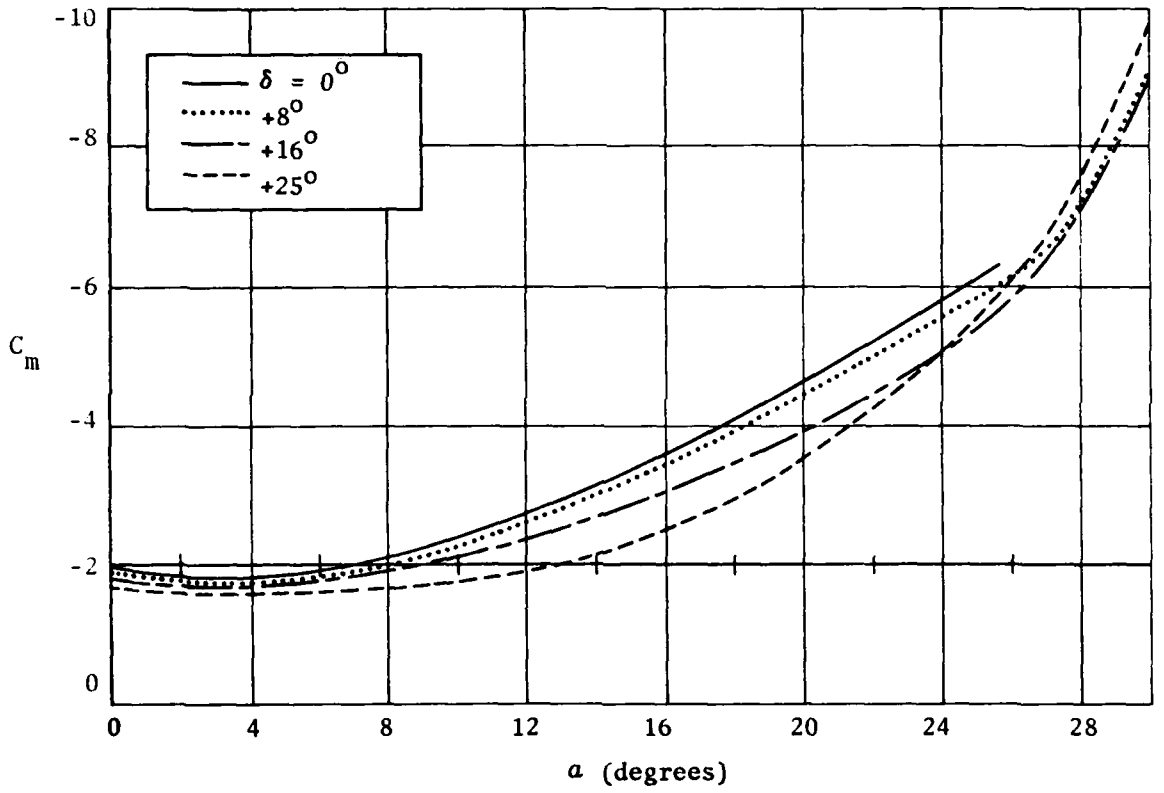

Figure 5(b)(Contd.).

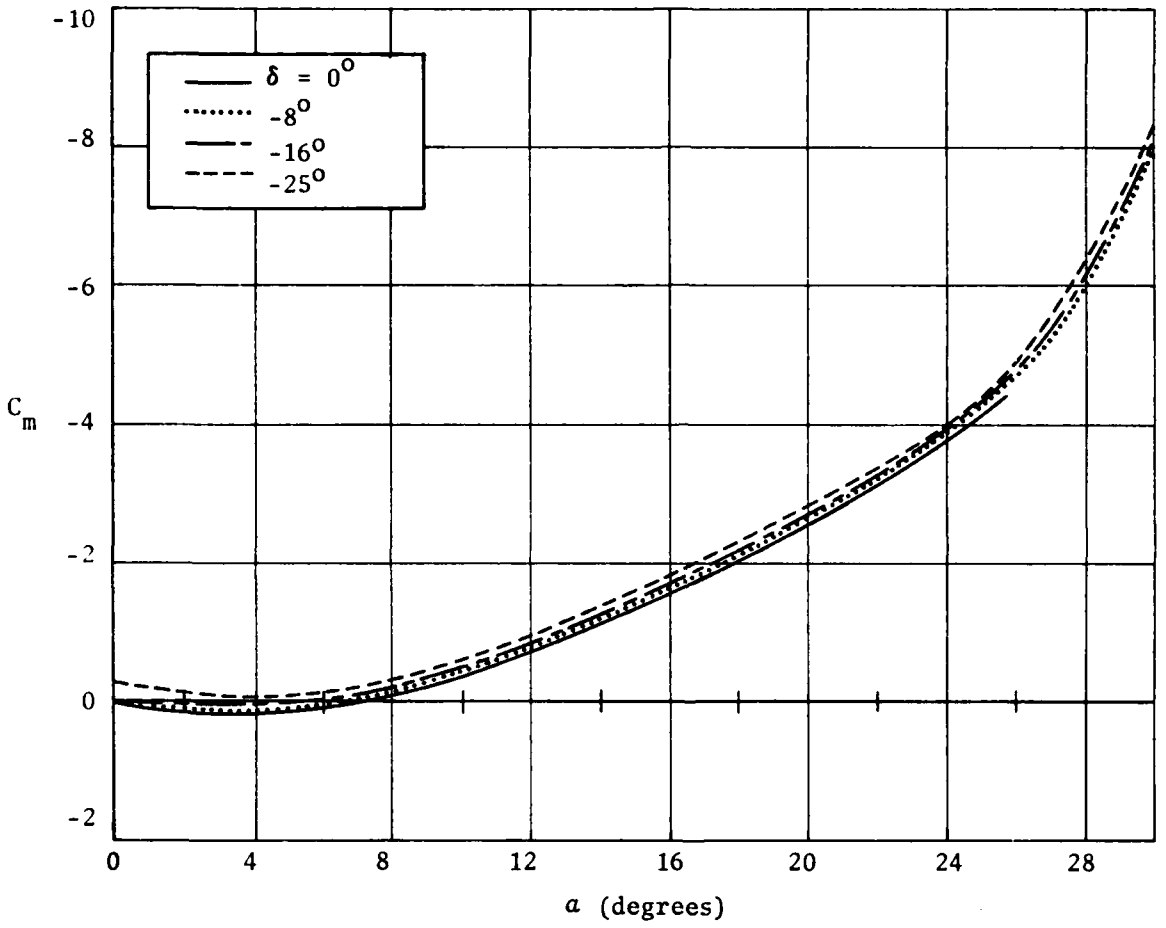

Figure 5(c). Pitching moment characteristics
M = 0.95

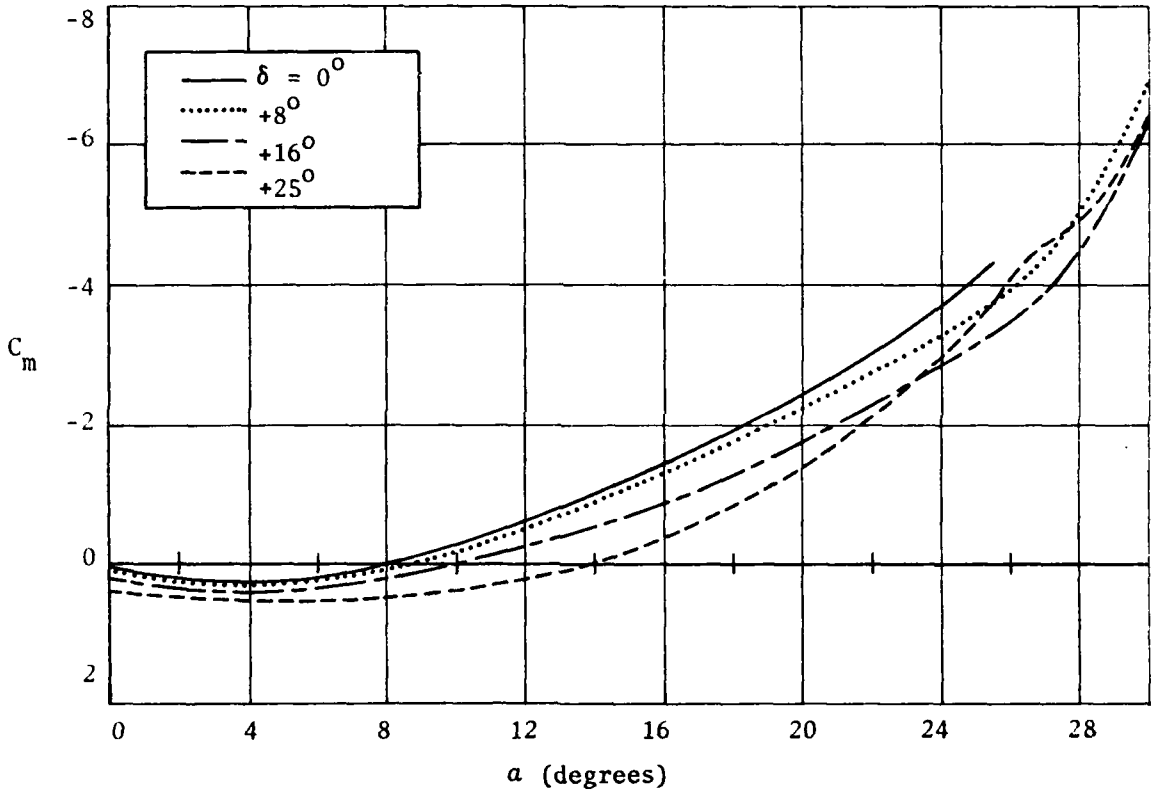

Figure 5(c)(Contd.).

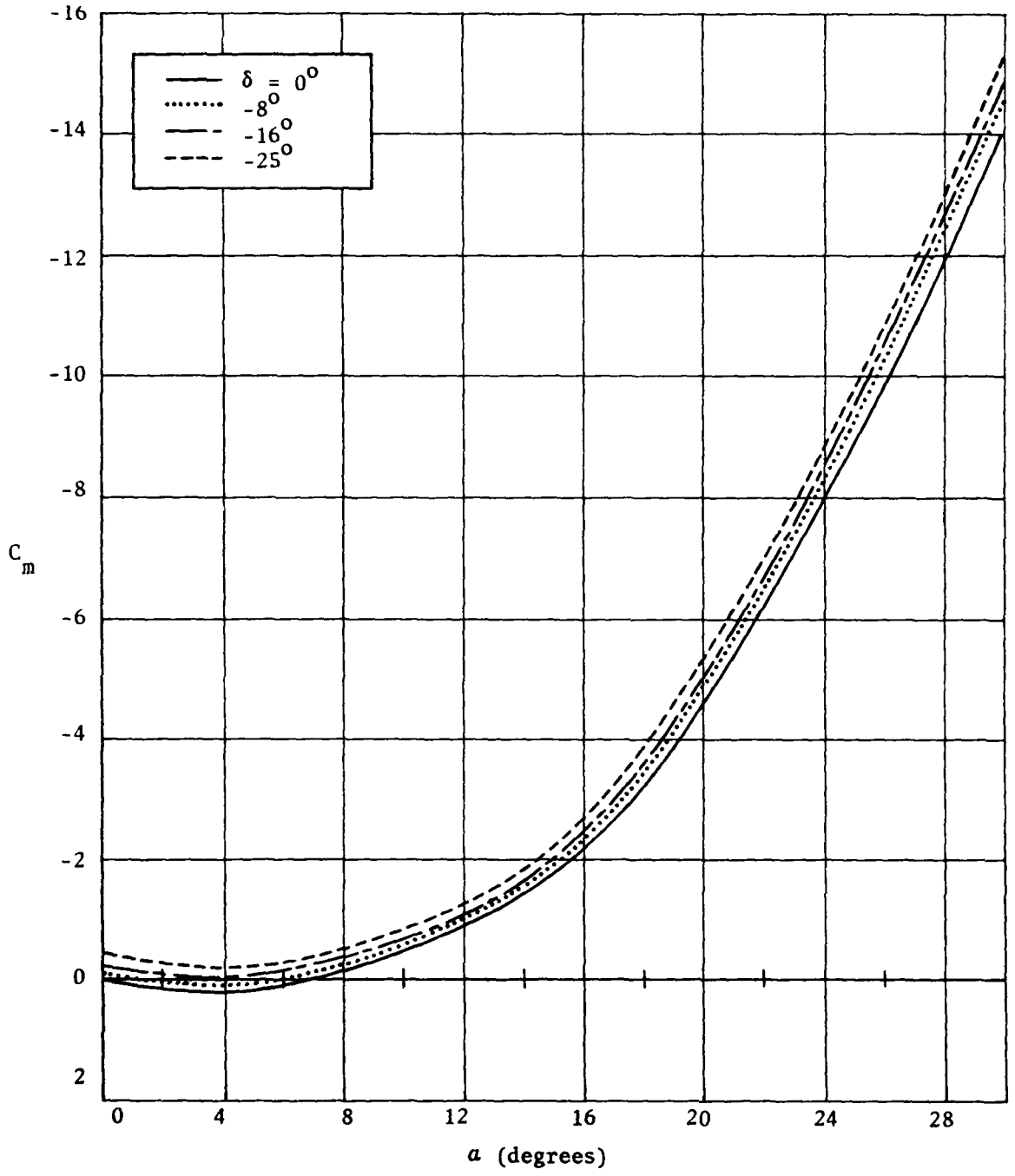

Figure 5(d). Pitching moment characteristics
M = 1.40

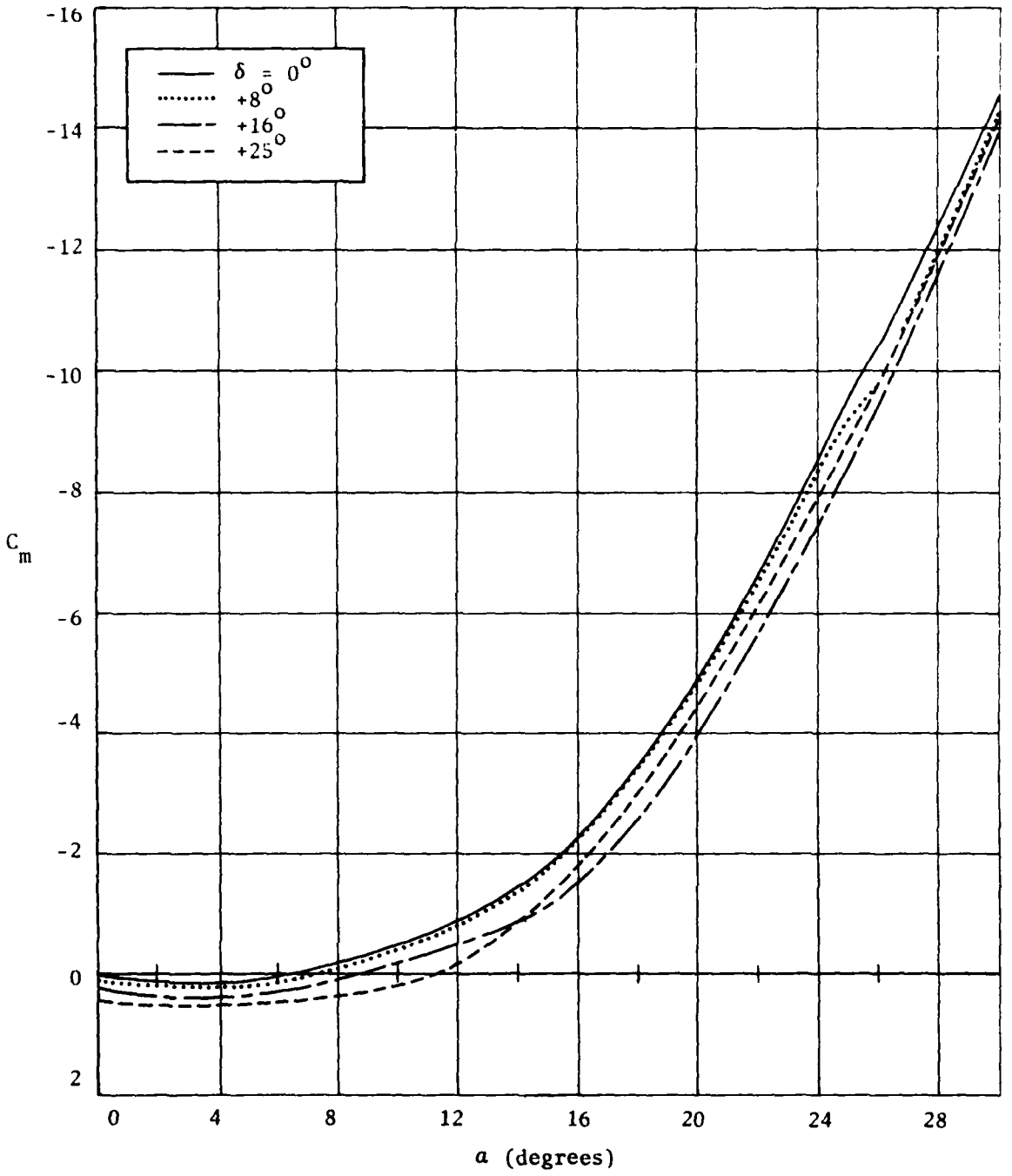

Figure 5(d)(Contd.).

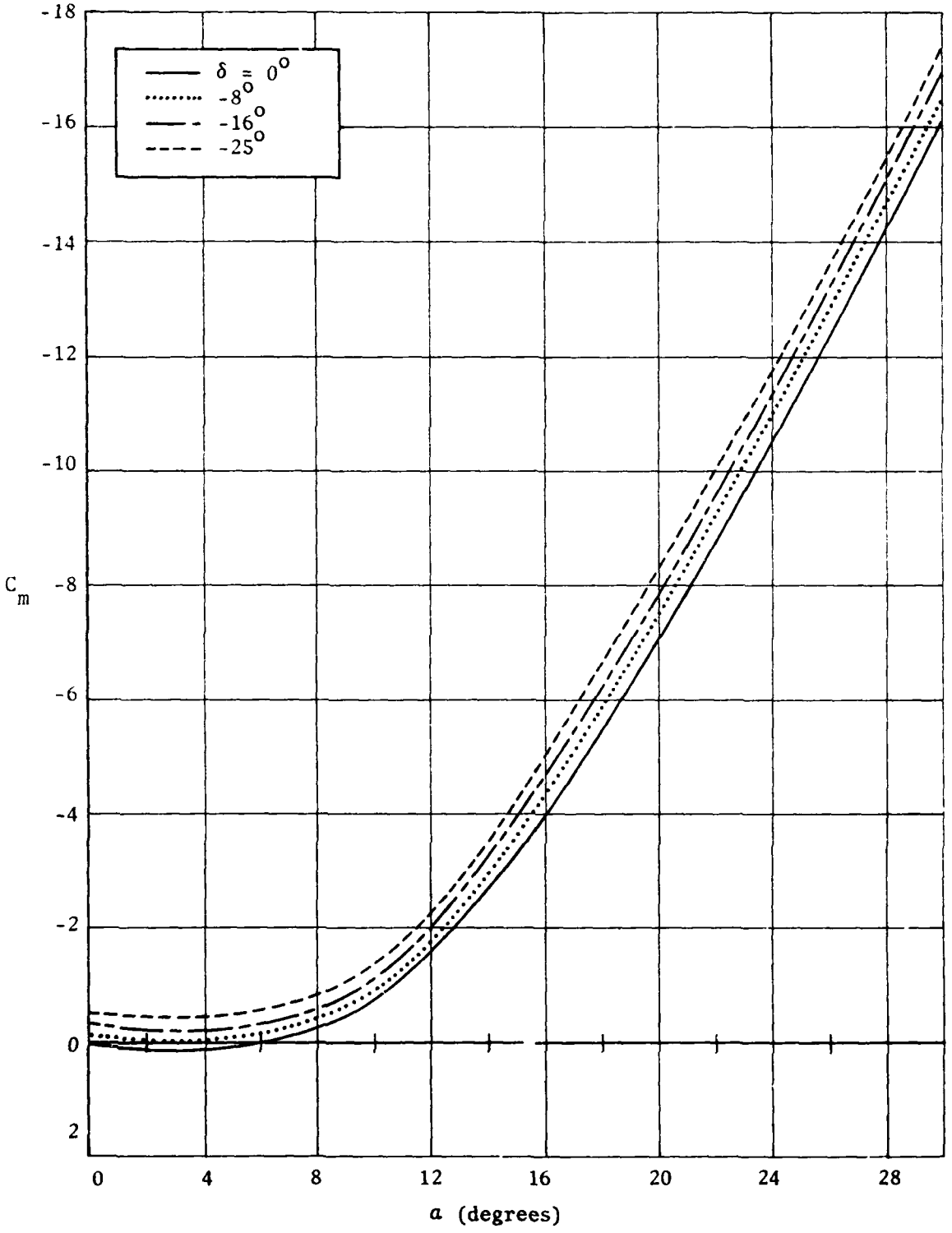

Figure 5(e). Pitching moment characteristics
M = 2.00

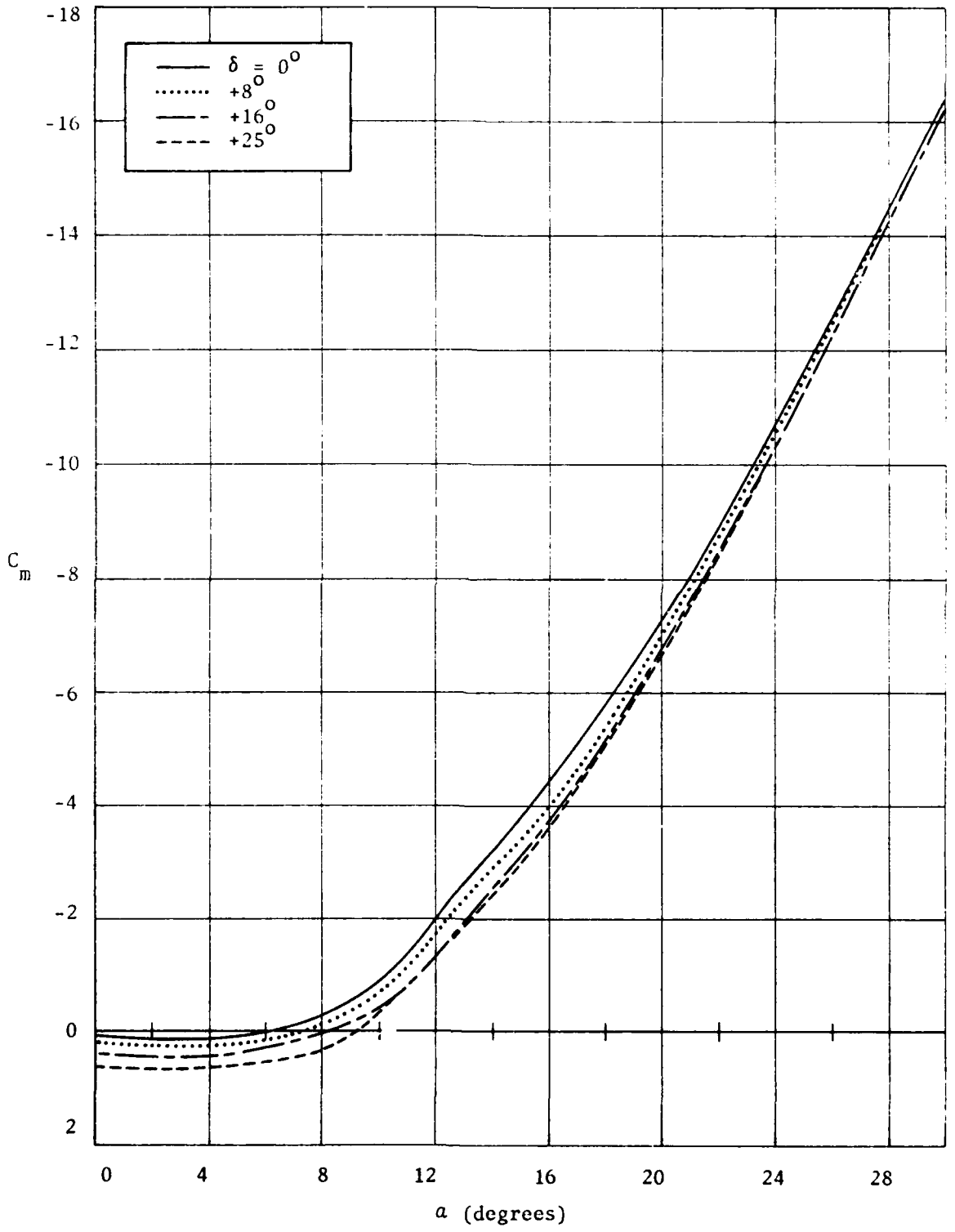

Figure 5(e)(Contd.).

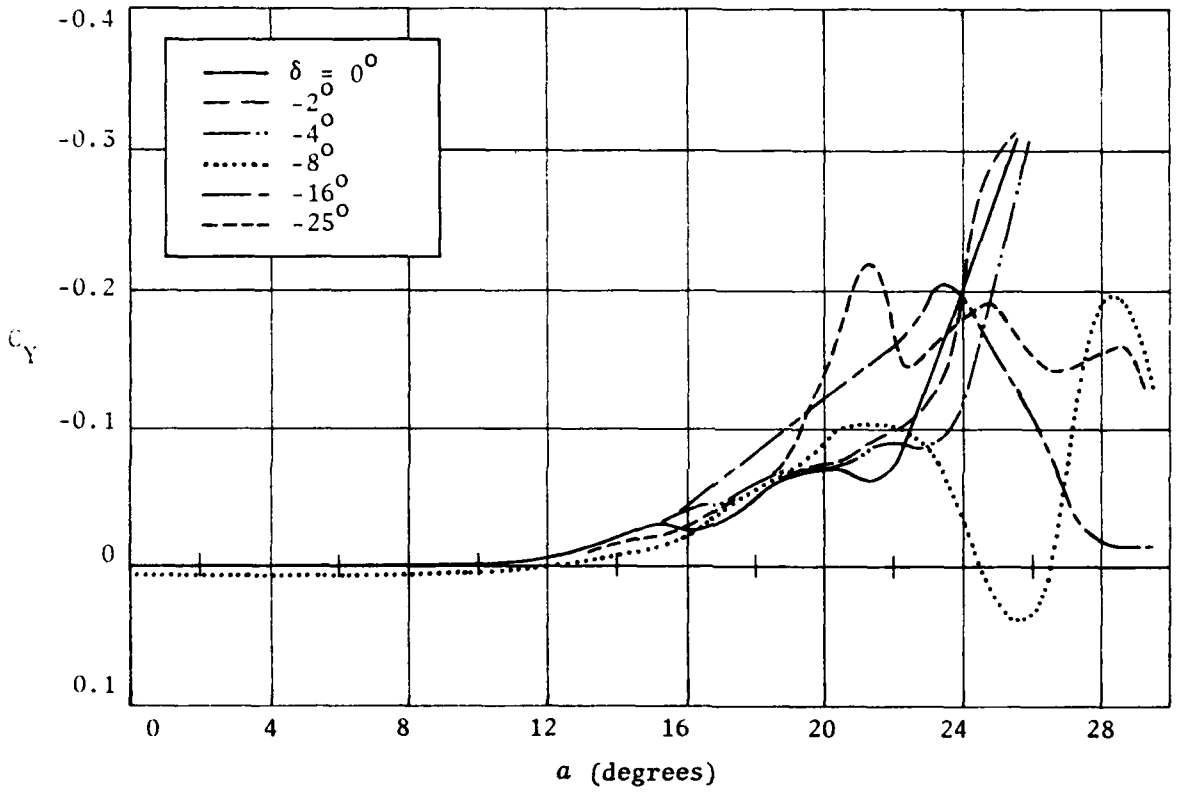

Figure 6(a). Side force characteristics
M = 0.80

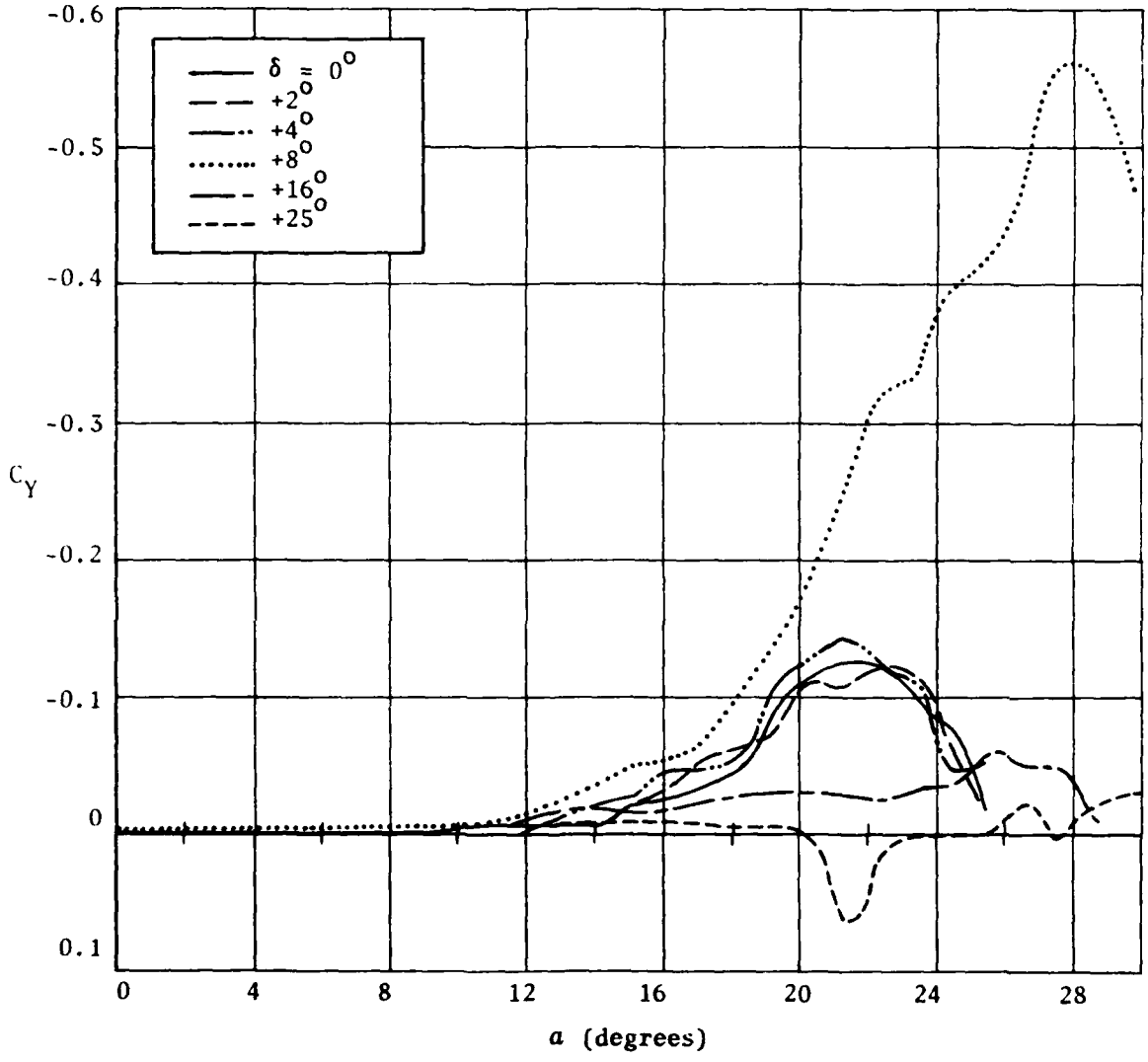

Figure 6(a)(Contd.).

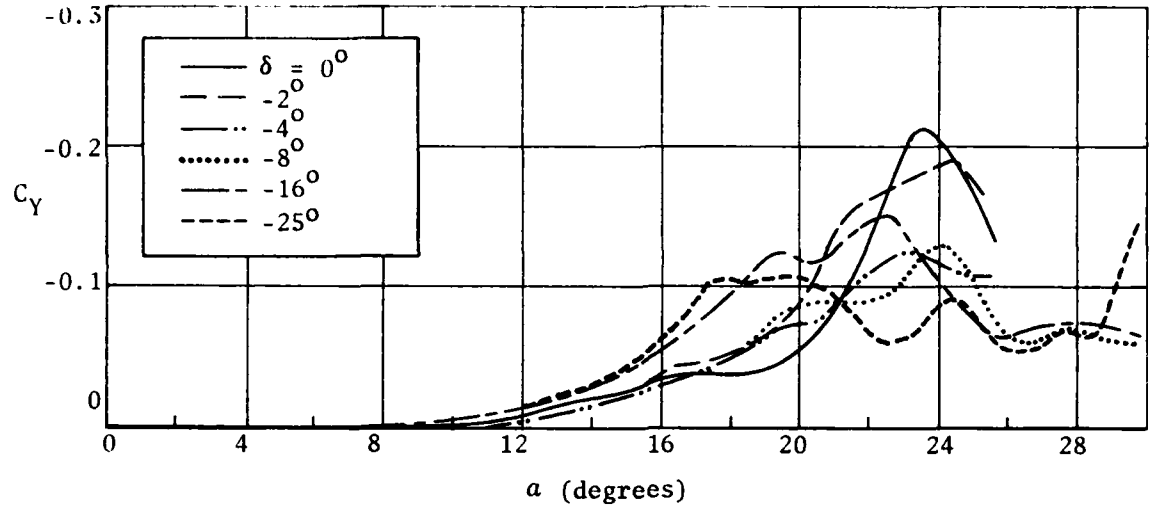

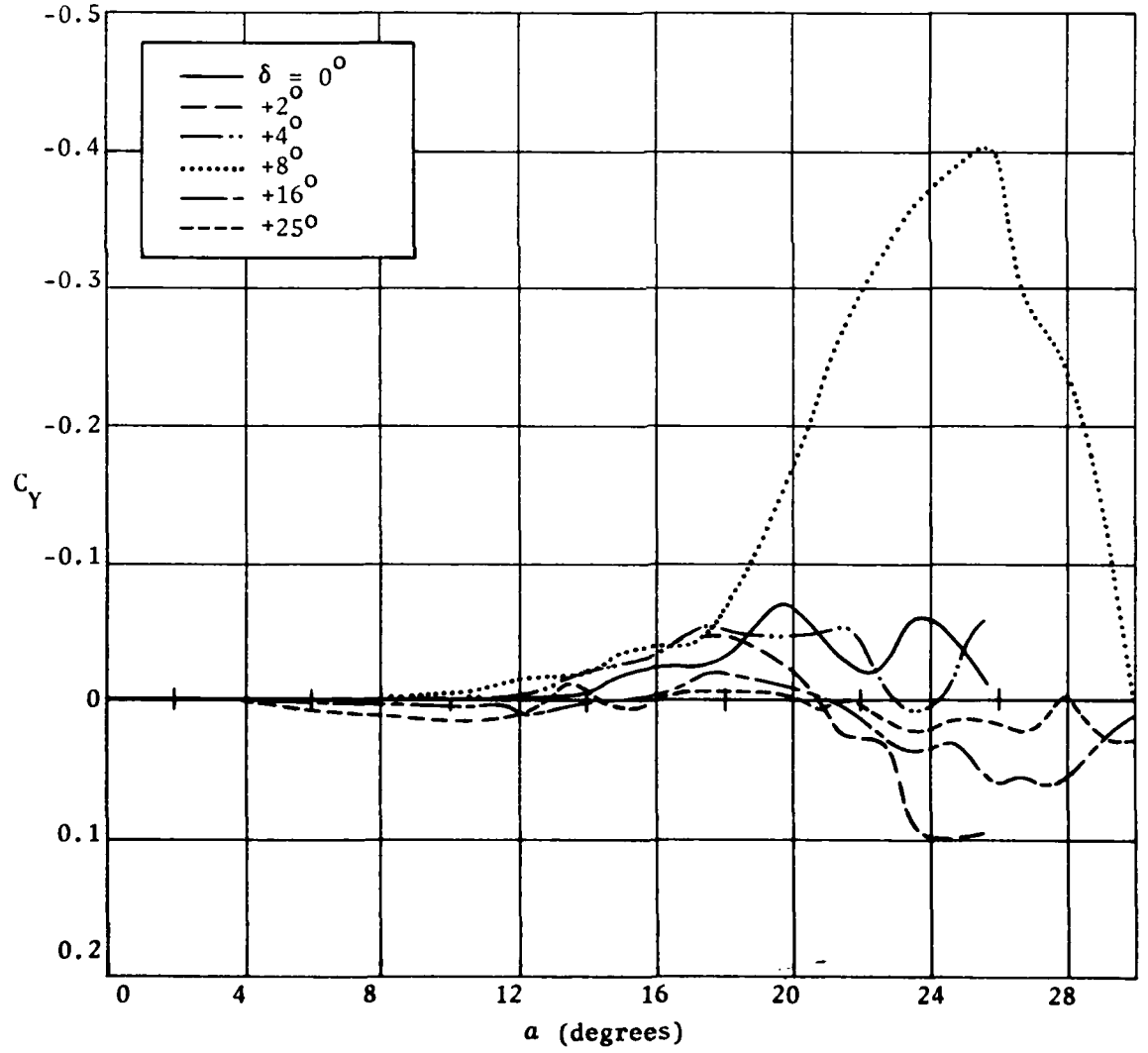

Figure 6(b). Side force characteristics
M = 0.90

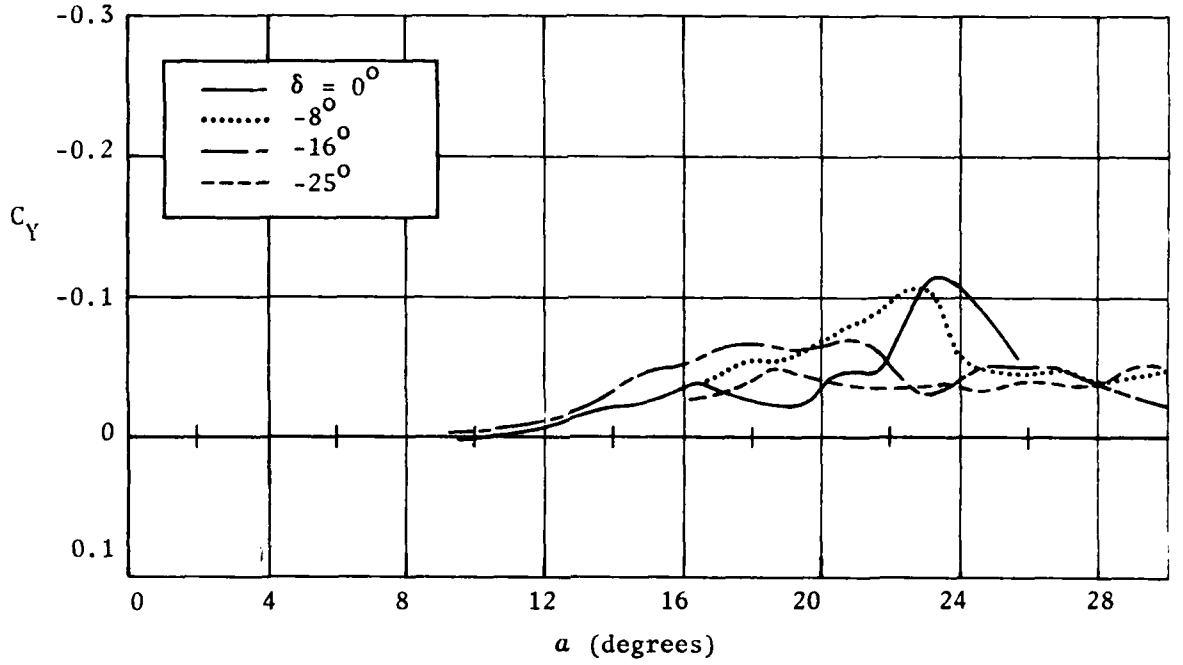

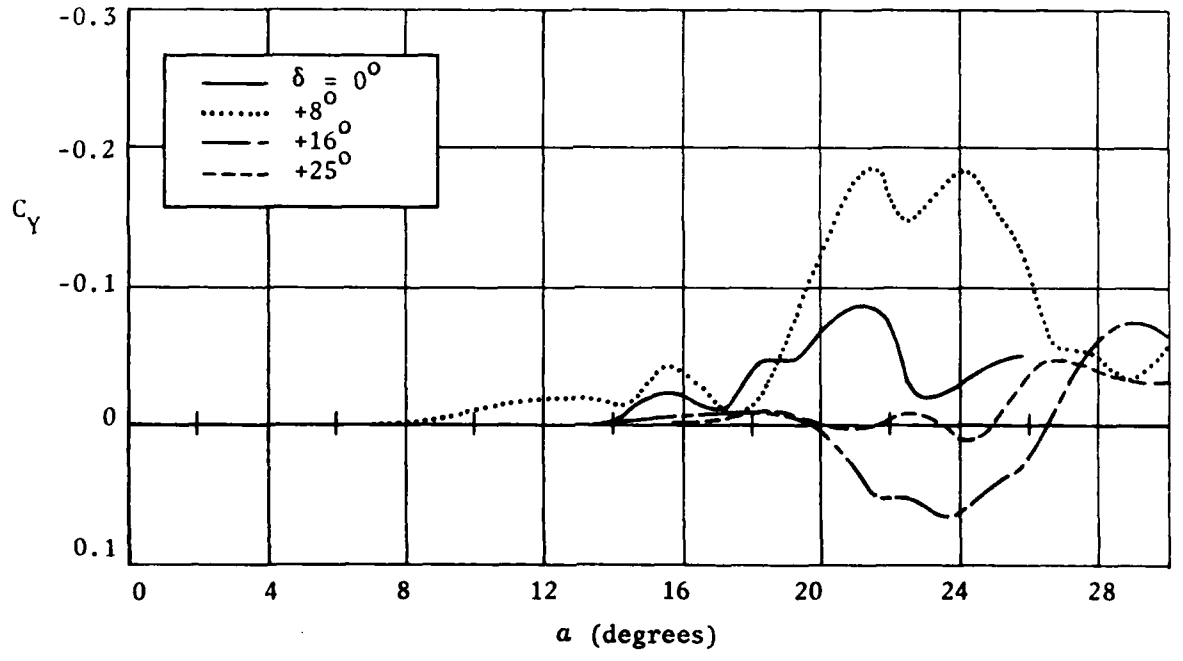

Figure 6(c). Side force characteristics
M = 0.95

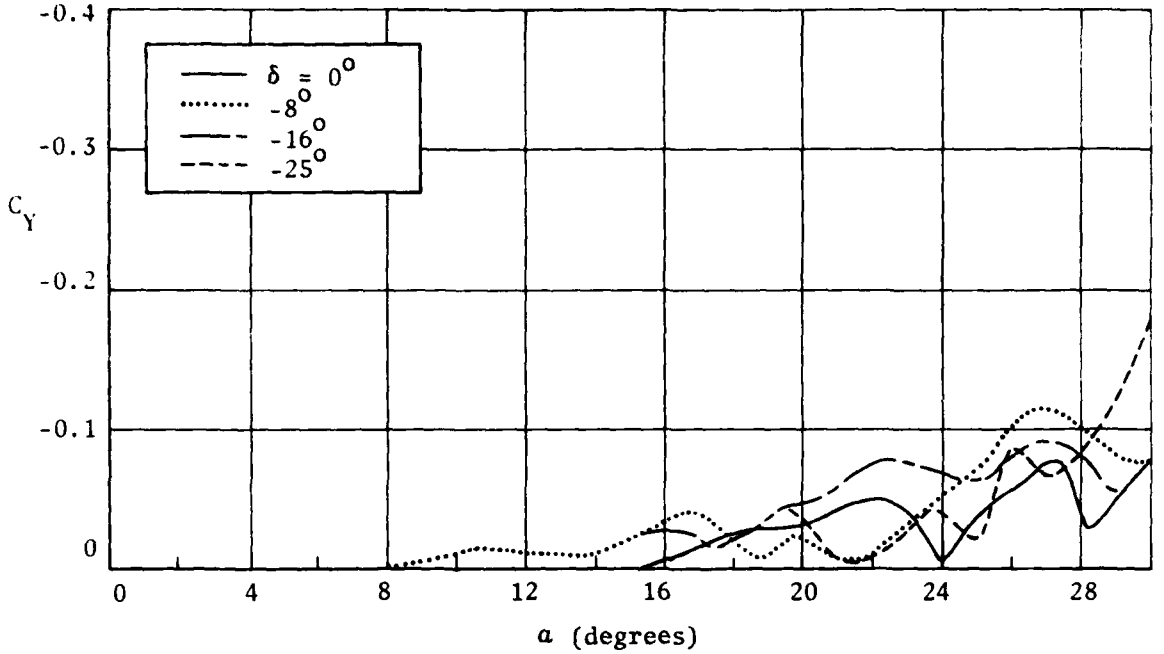

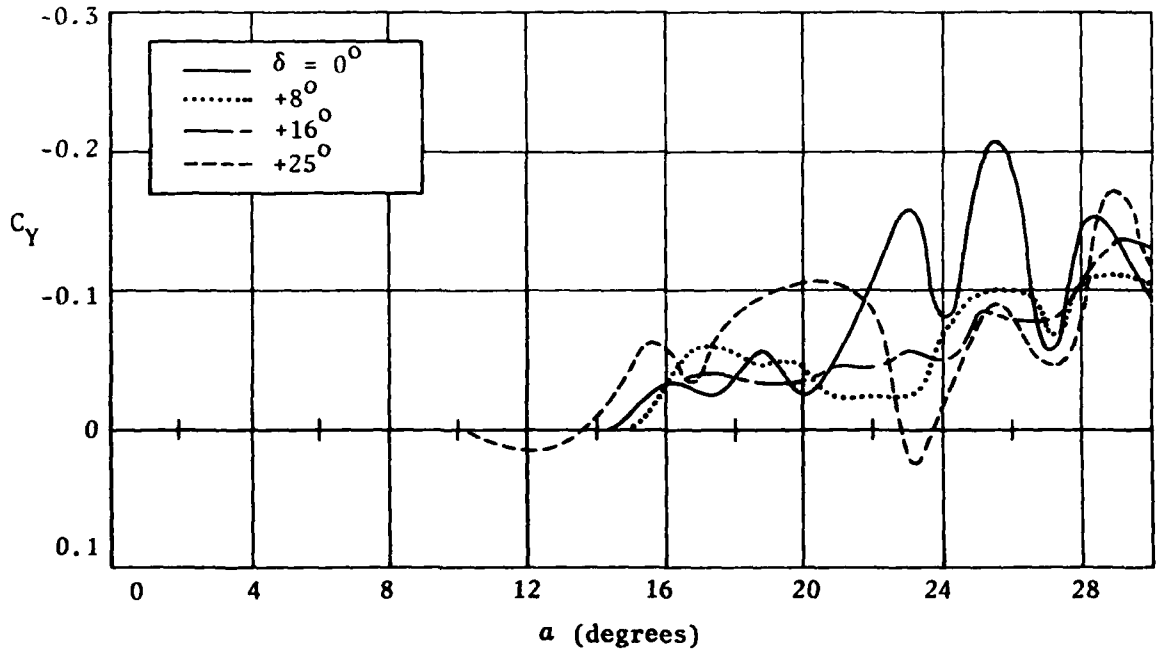

Figure 6(d). Side force characteristics
M = 1.40

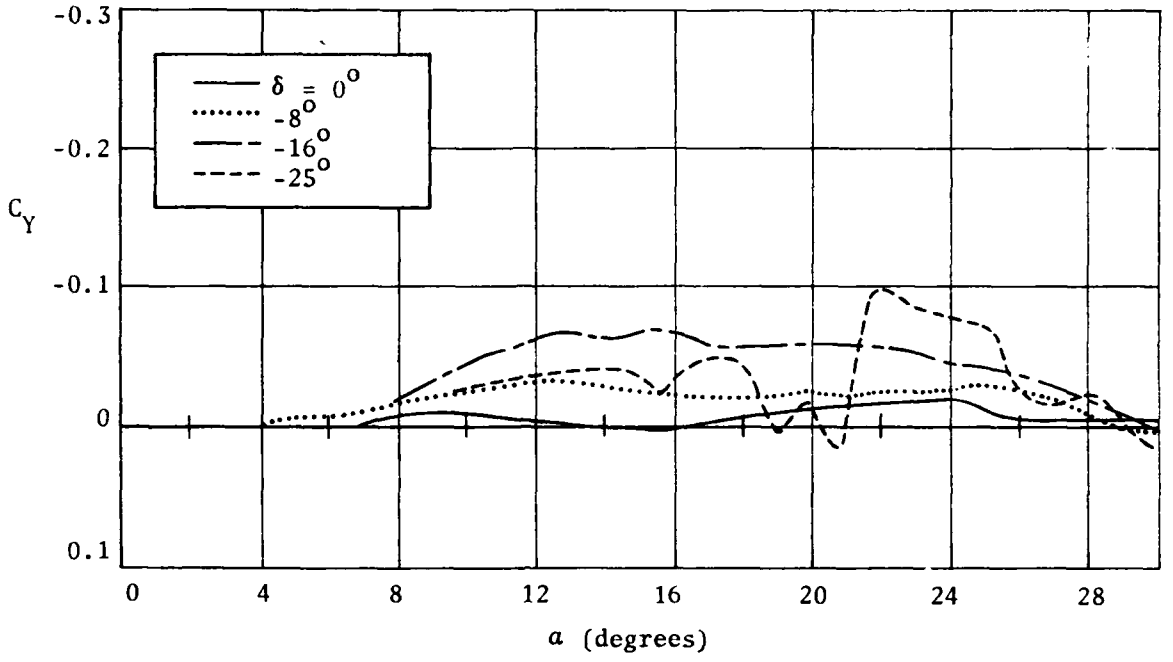

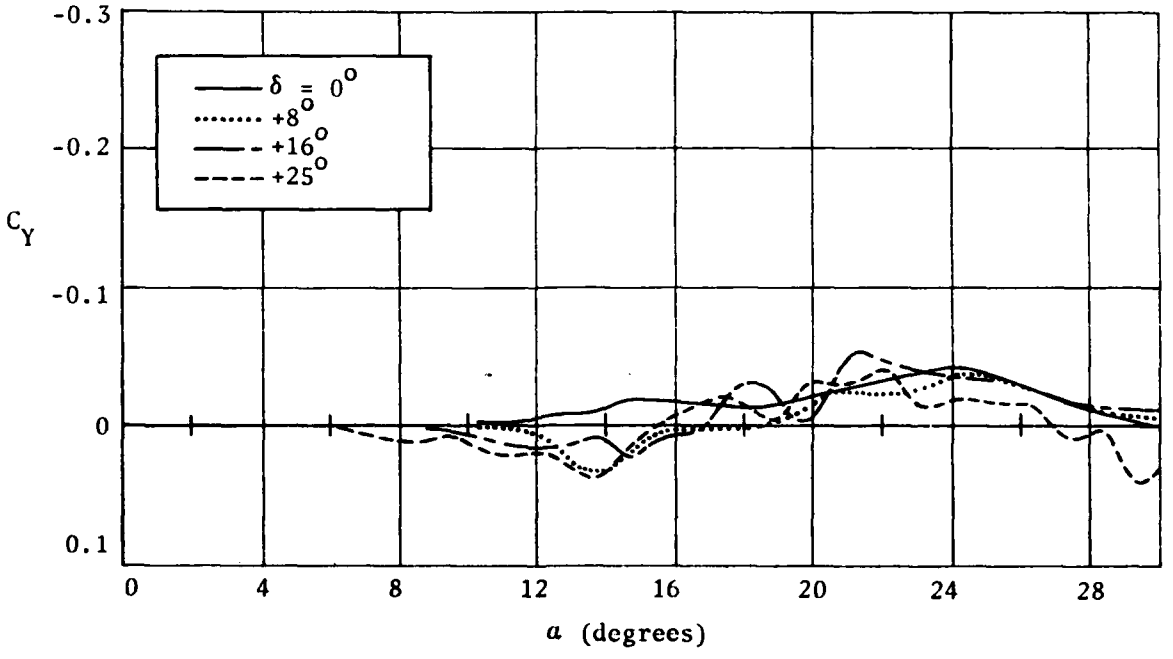

Figure 6(e). Side force characteristics
M = 2.00

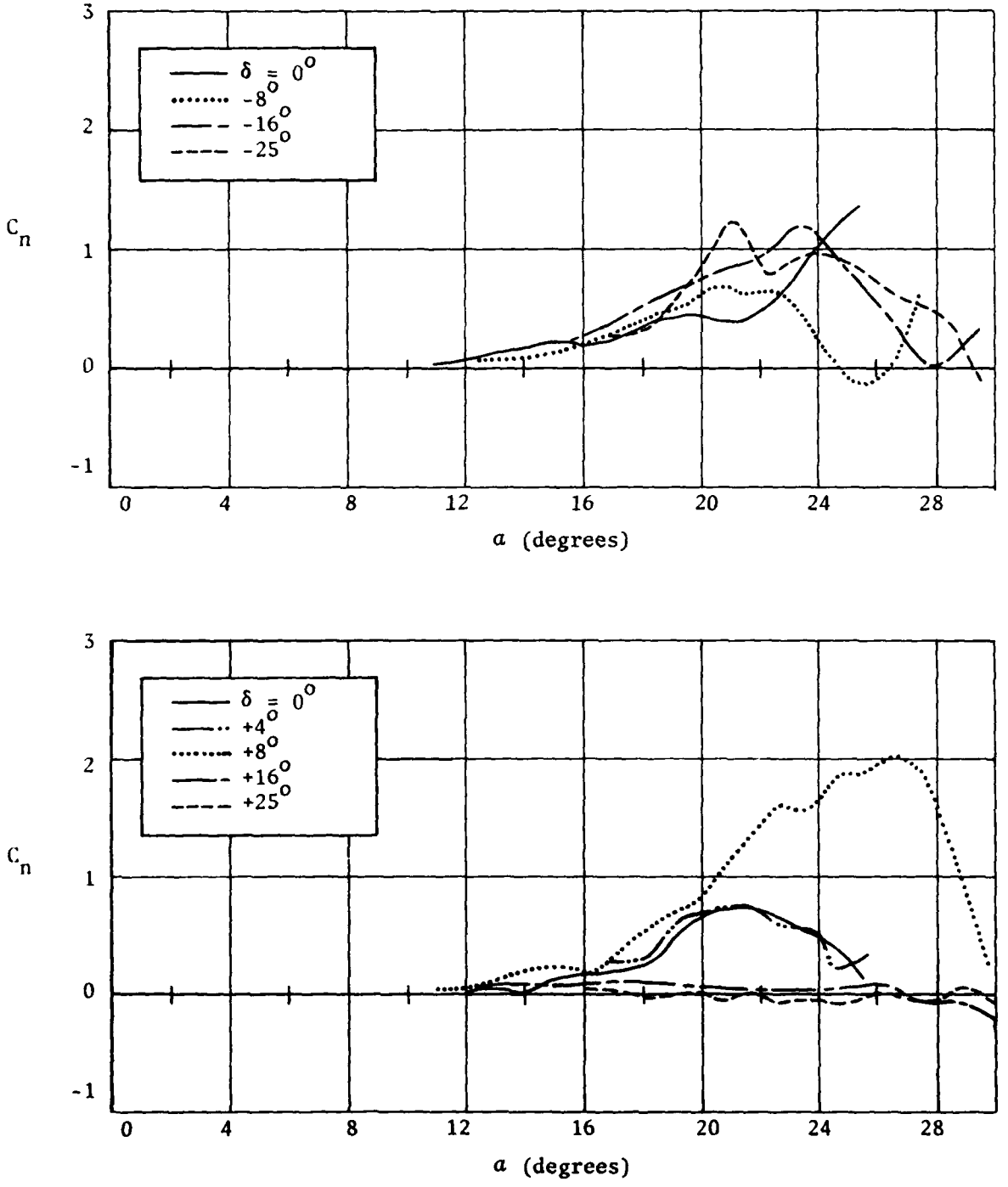

Figure 7(a). Yawing moment characteristics
M = 0.80

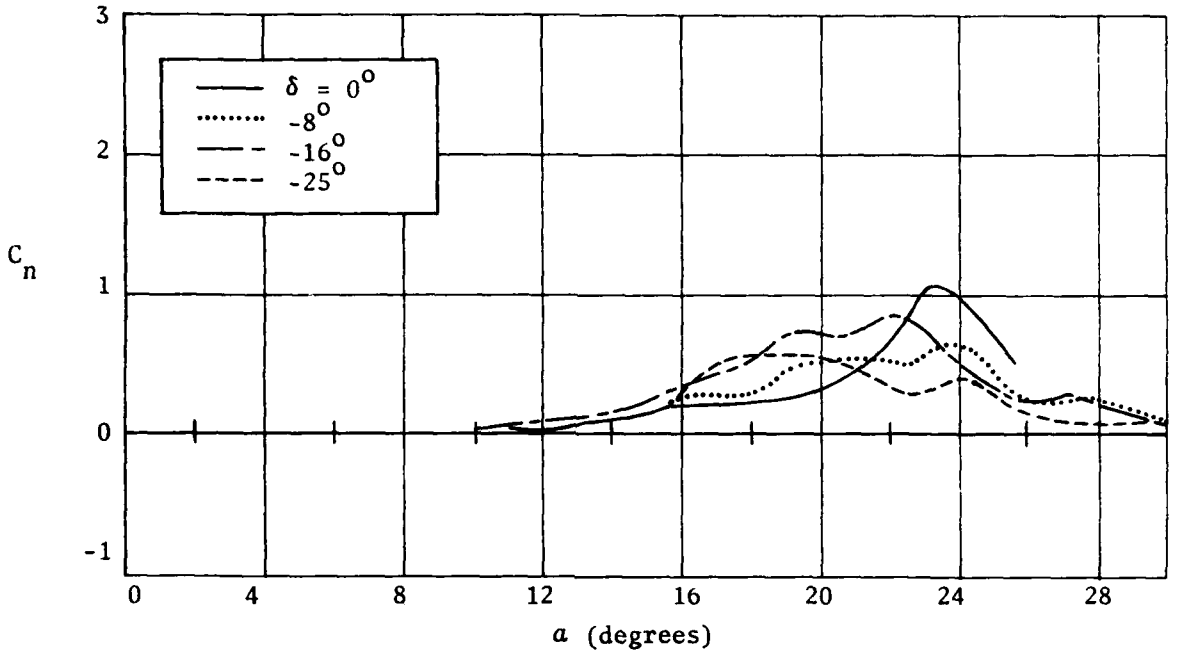

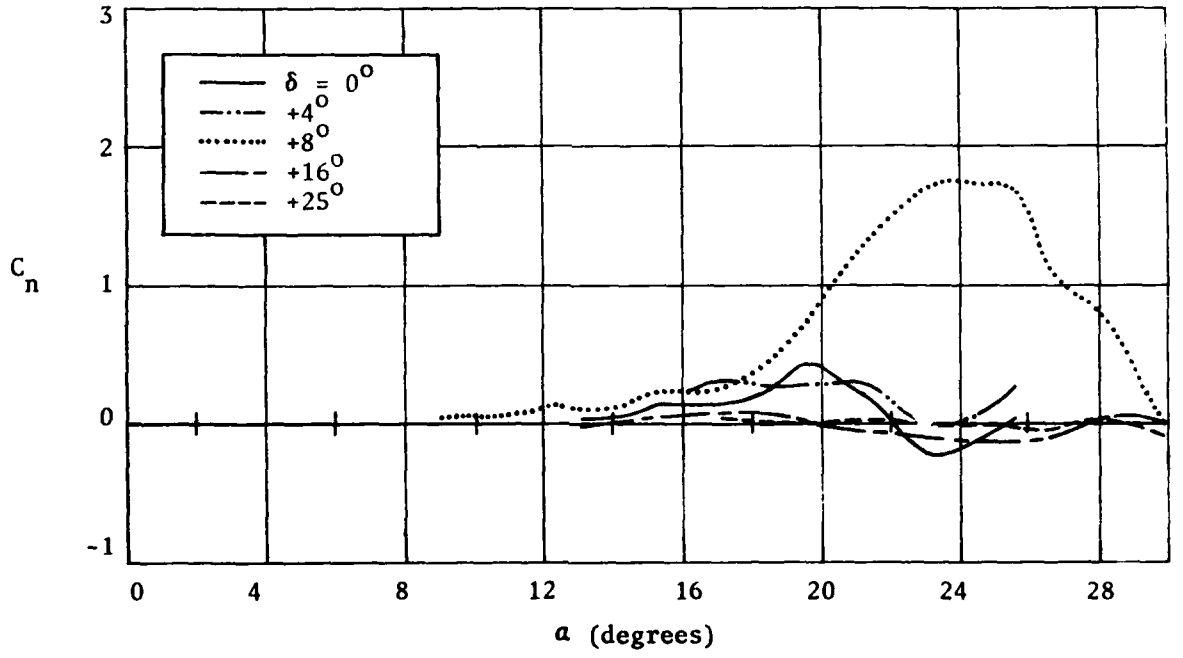

Figure 7(b). Yawing moment characteristics
M = 0.90

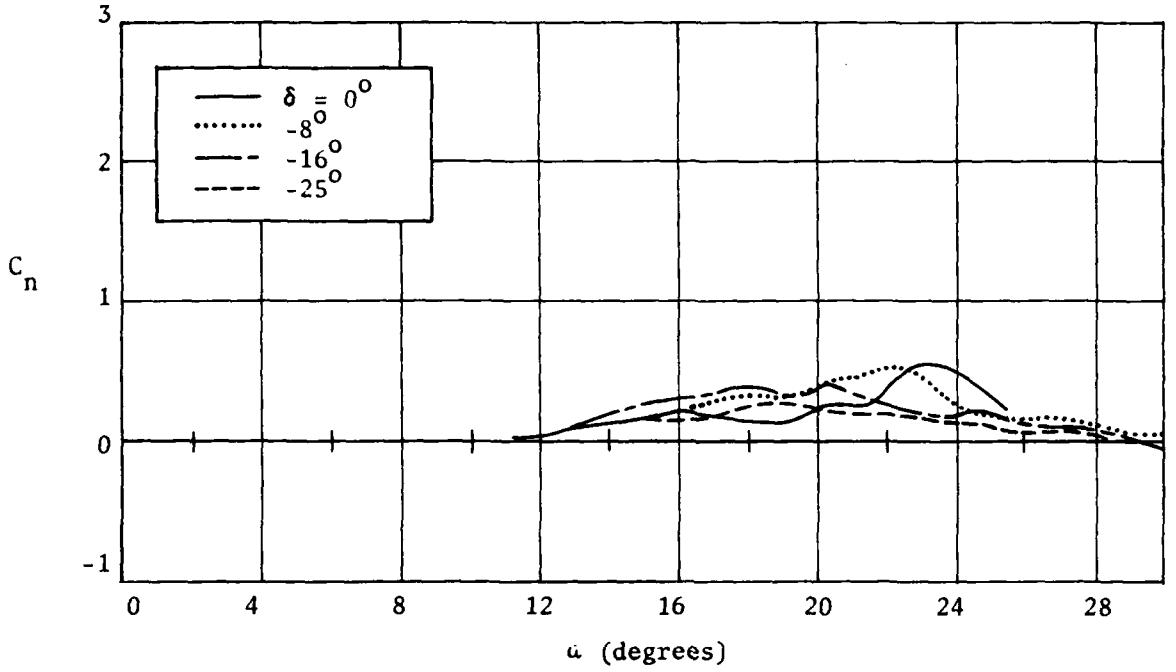

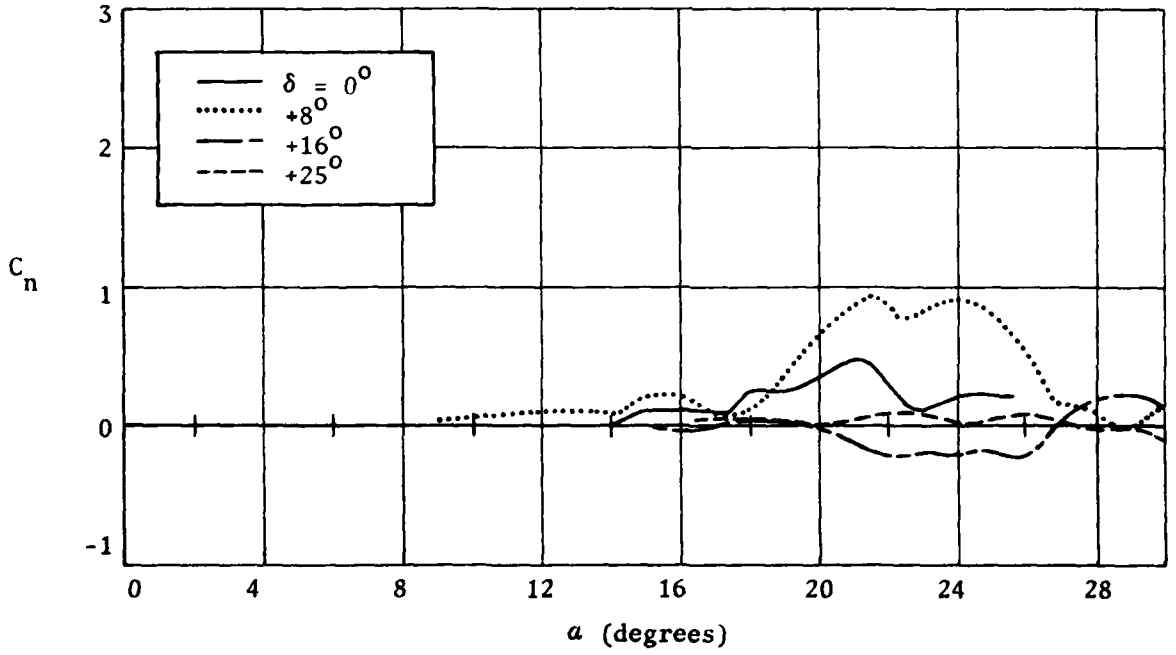

Figure 7(c). Yawing moment characteristics
M = 0.95

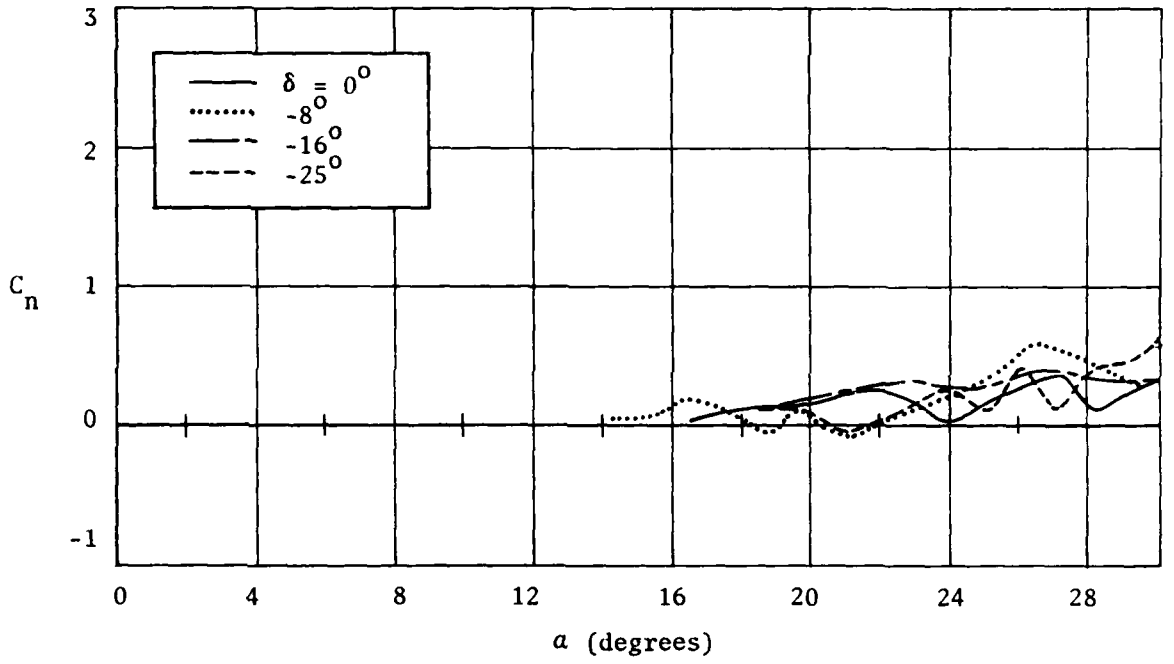

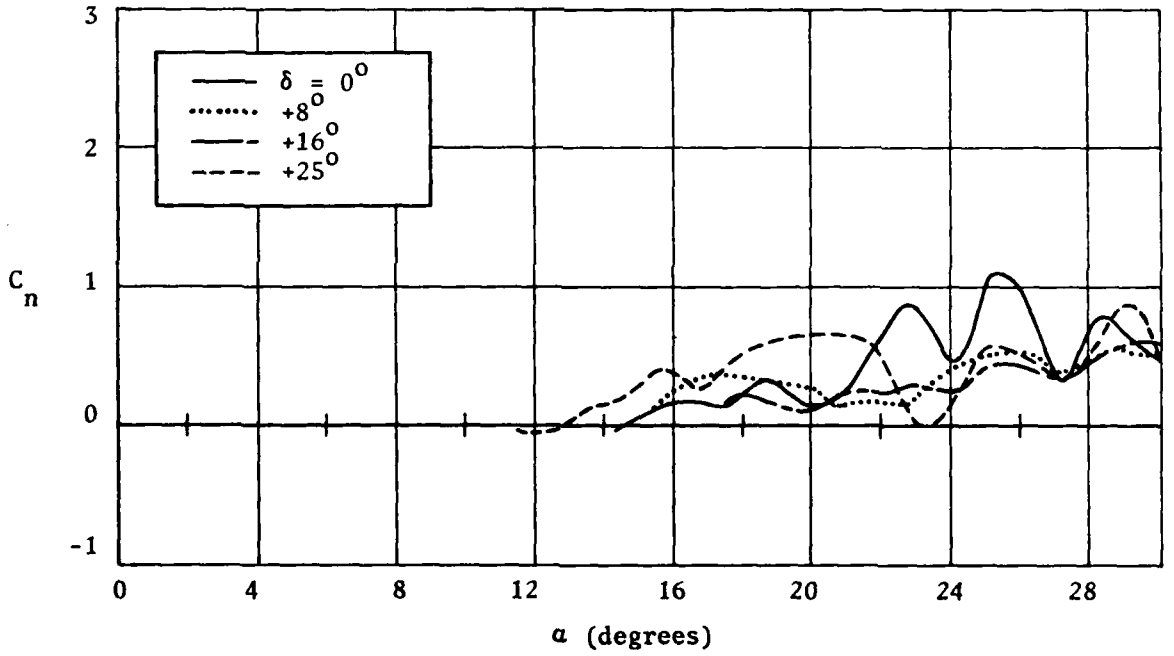

Figure 7(d). Yawing moment characteristics
M = 1.40

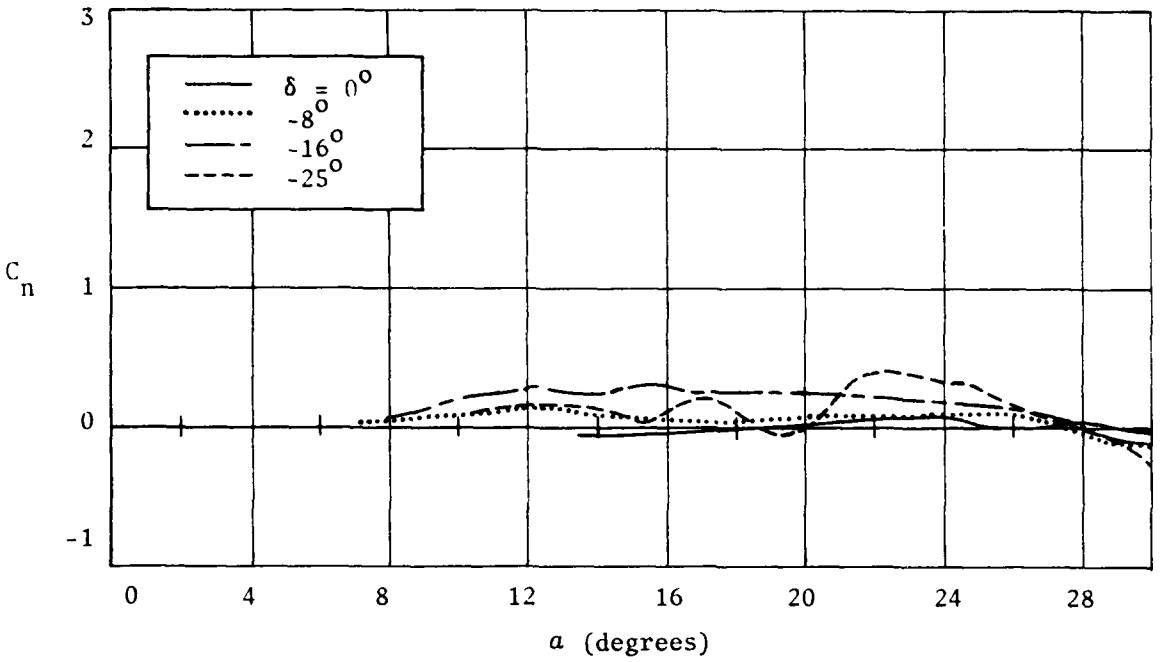

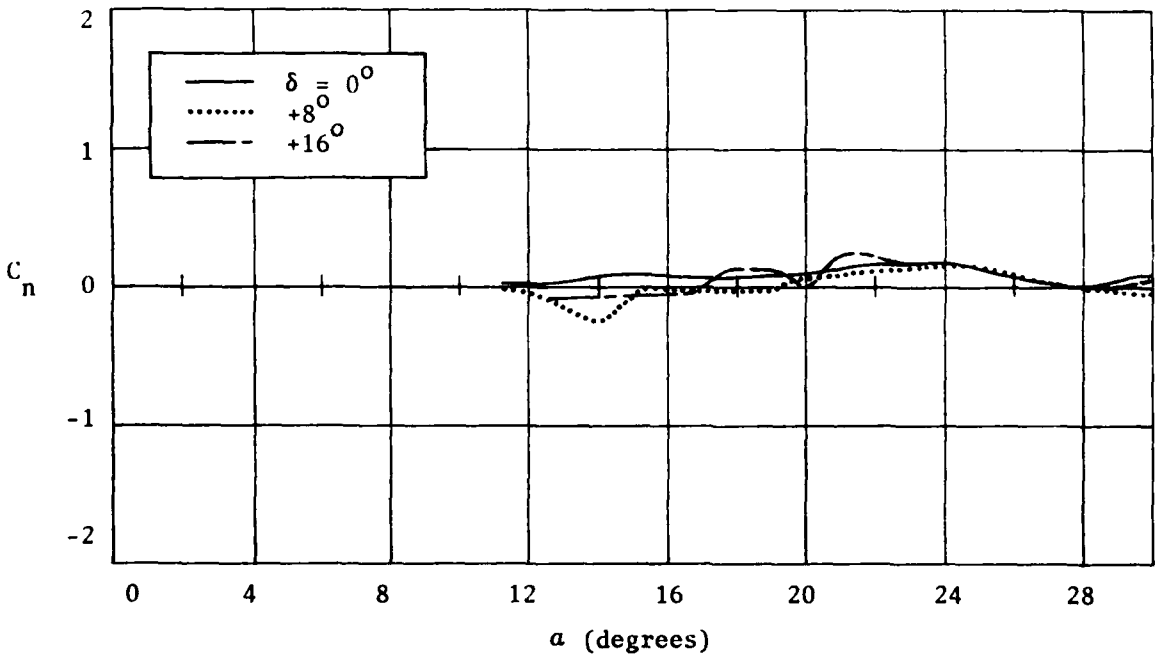

Figure 7(e). Yawing moment characteristics
M = 2.00

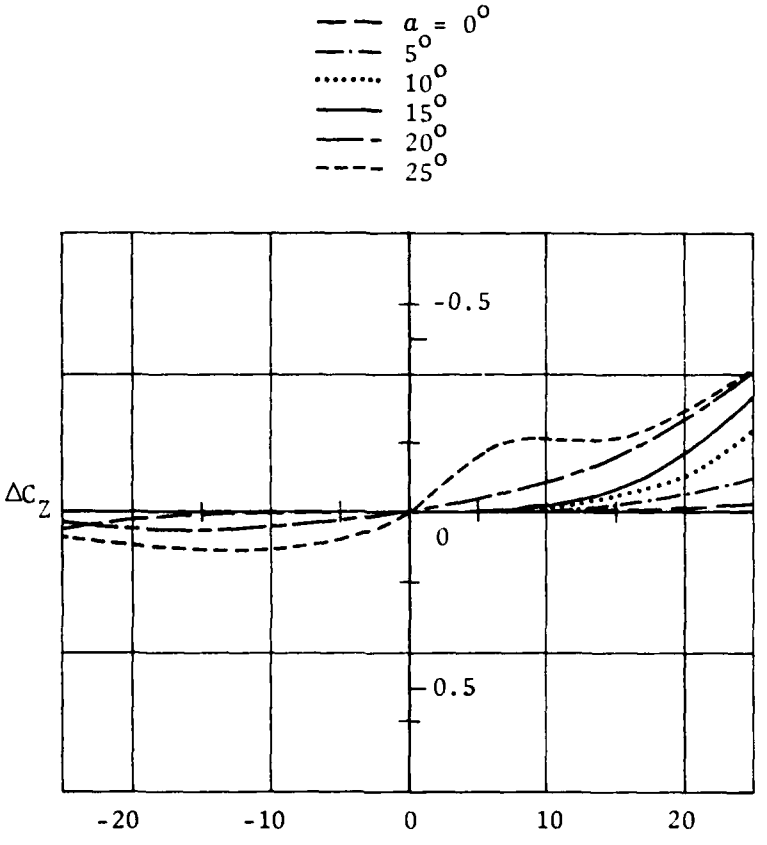

(a) M = 0.80

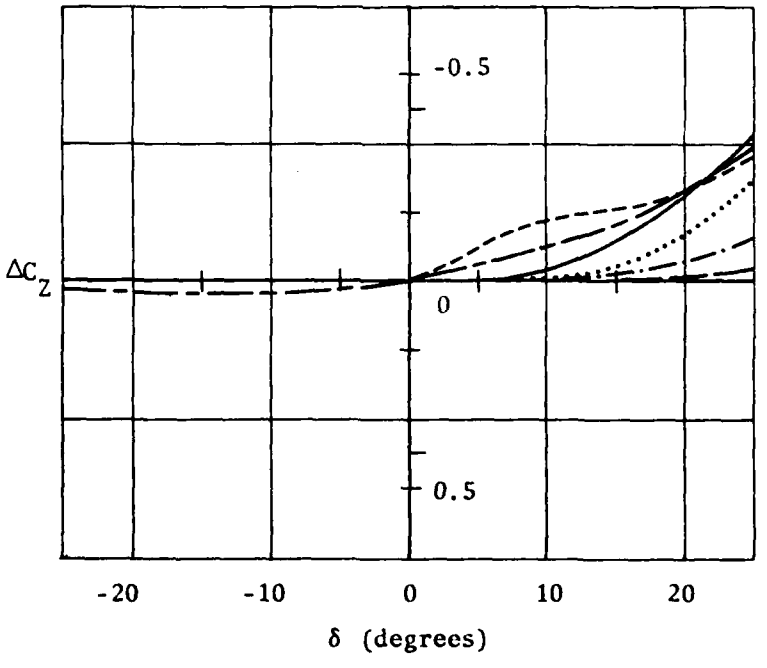

(b) M = 0.90

Figure 8. Increment in normal force coefficient due to nose deflection

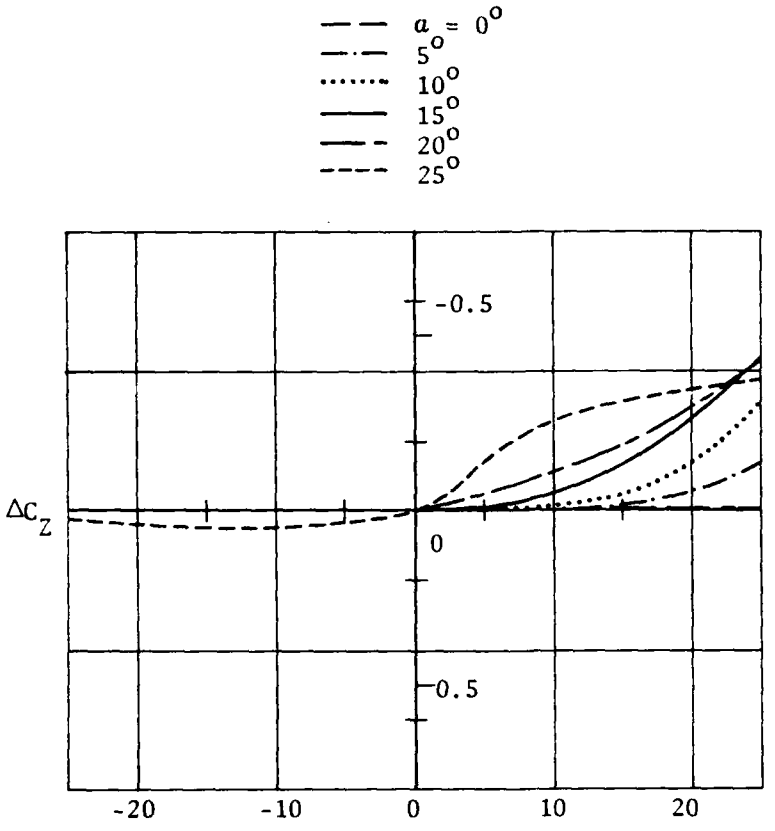

(c) M = 0.95

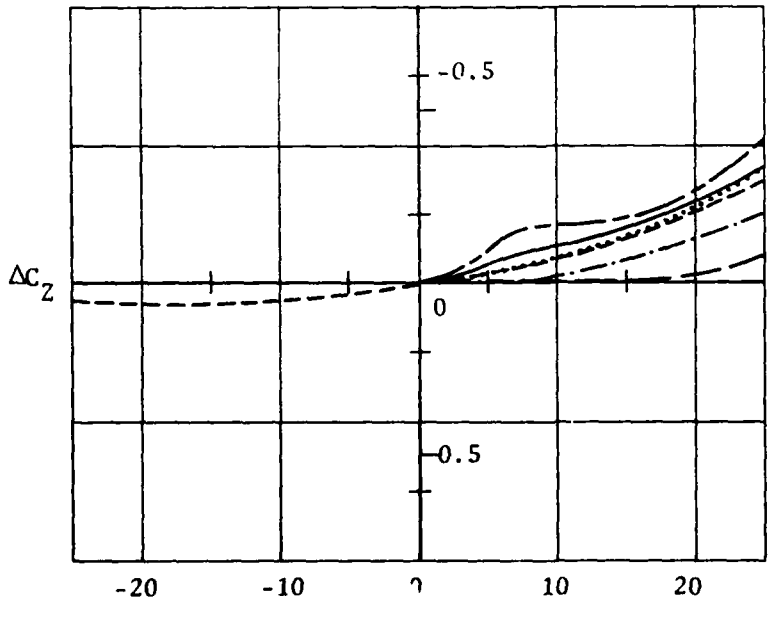

(d) M = 1.40

Figure 8(Contd.).

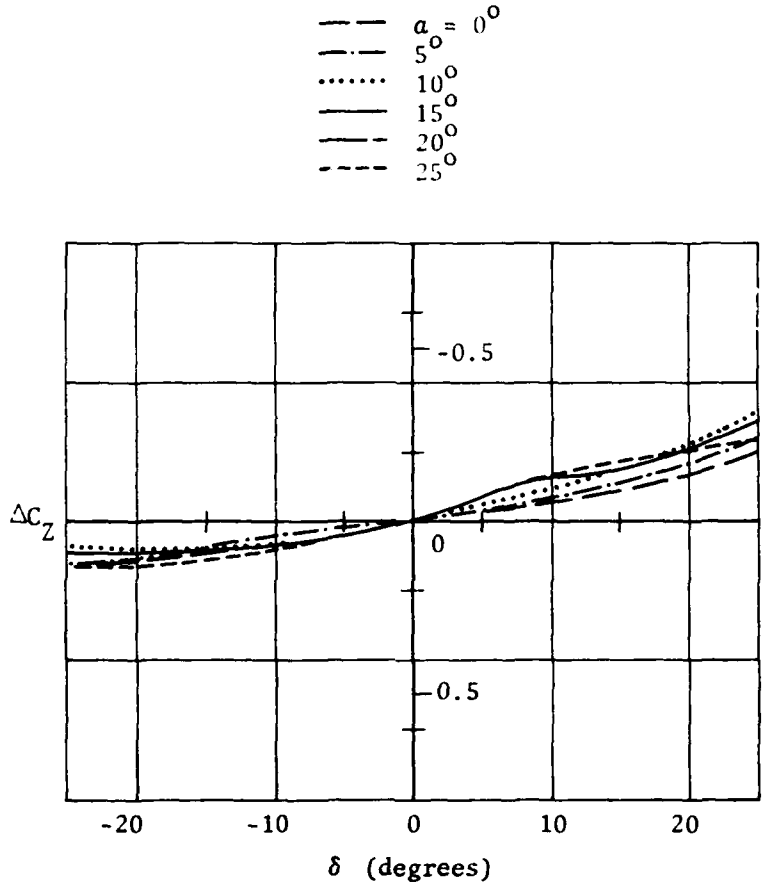

(e) M = 2.00

Figure 8(Contd.).

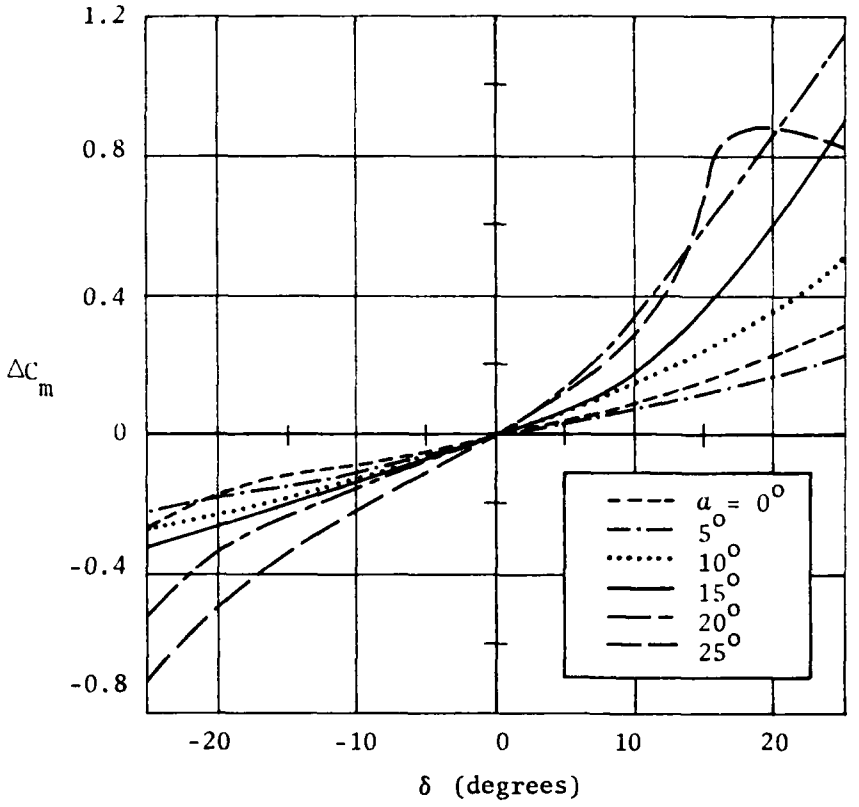

(a) M = 0.80

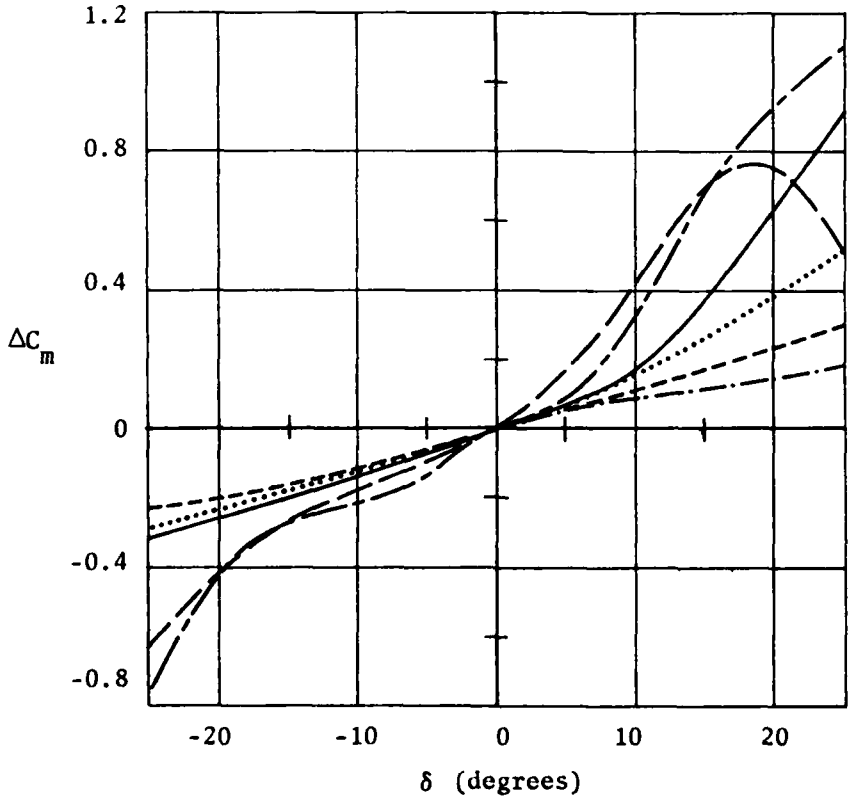

(b) M = 0.90

Figure 9. Increment in pitching moment coefficient due to nose deflection

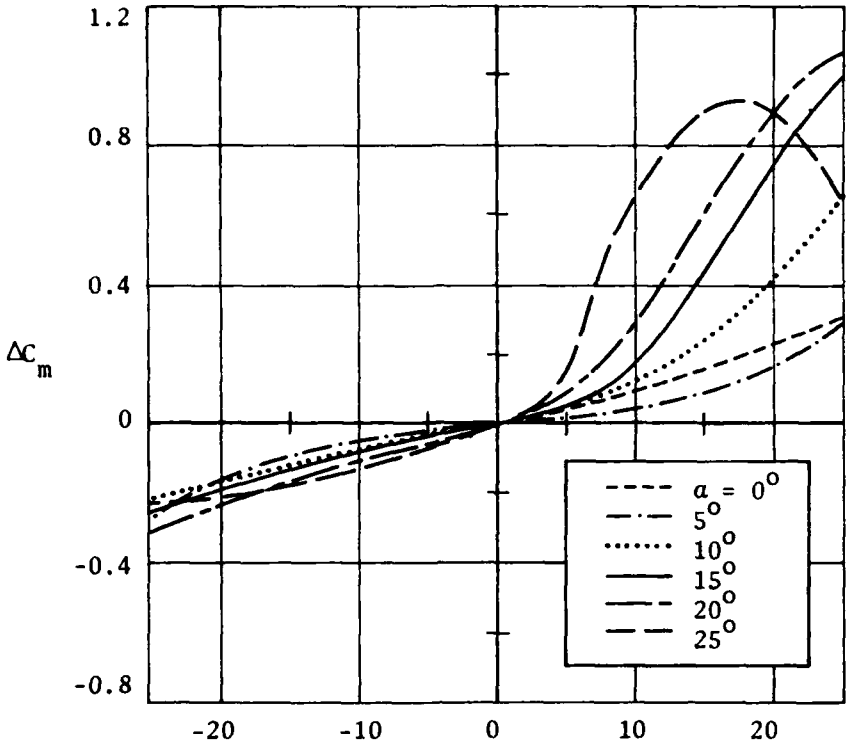

(c) M = 0.95

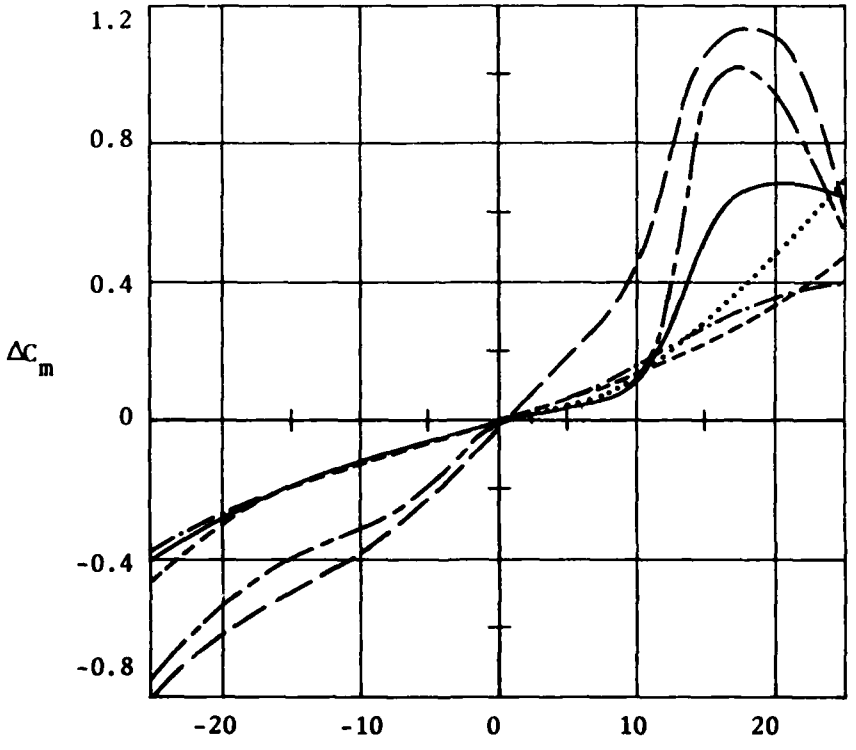

(d) M = 1.40

Figure 9(Contd.).

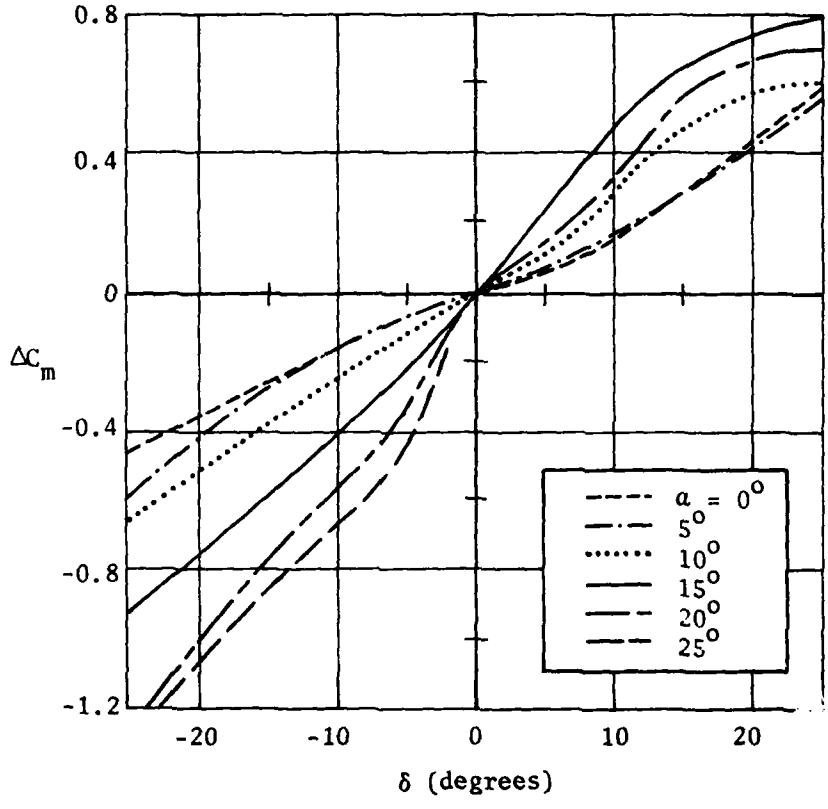

(e) M = 2.00

Figure 9(Contd.).

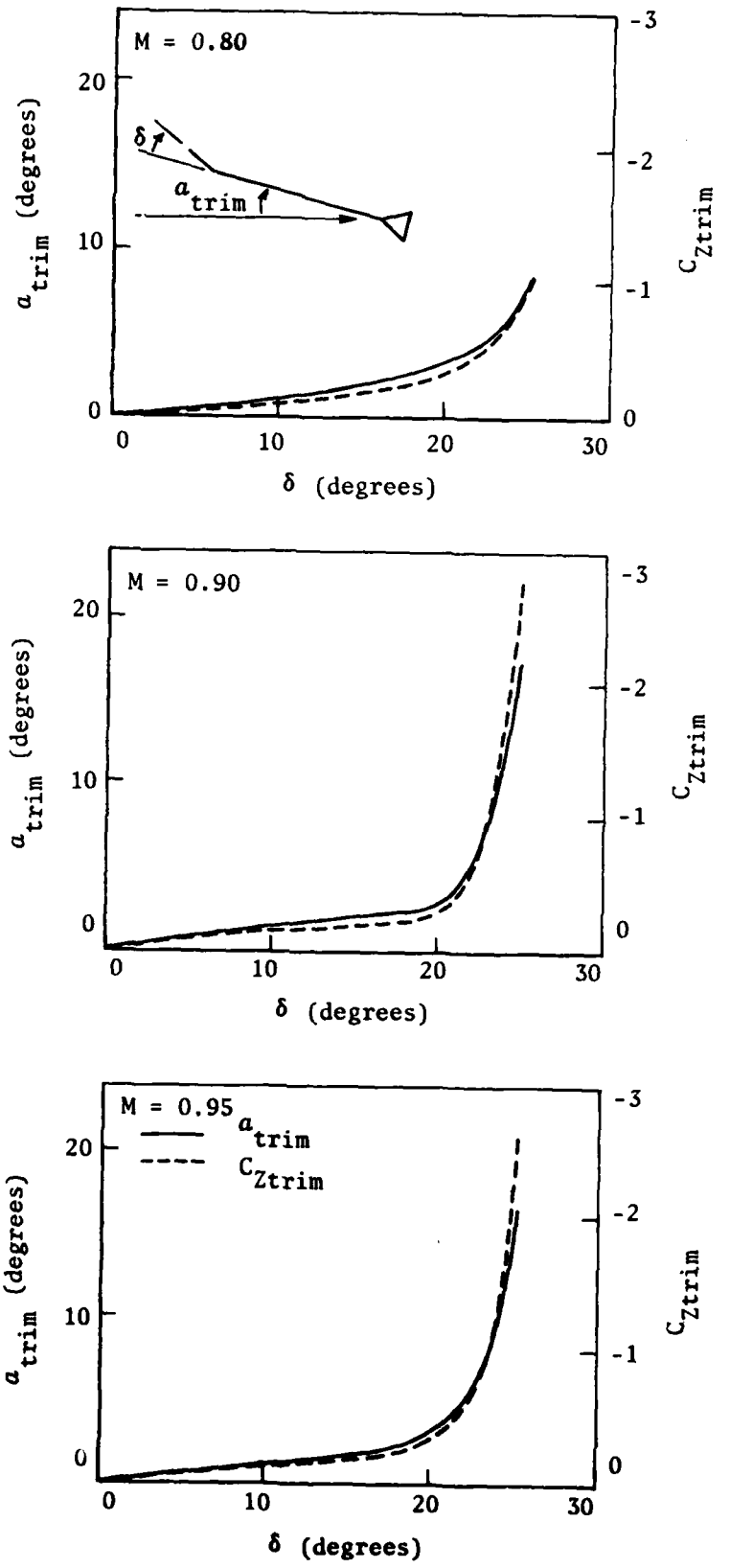

Figure 10. Trim curves for $\frac{L}{d}$ = 10.71 ogive-cylinder with stabilizer and deflectable nose

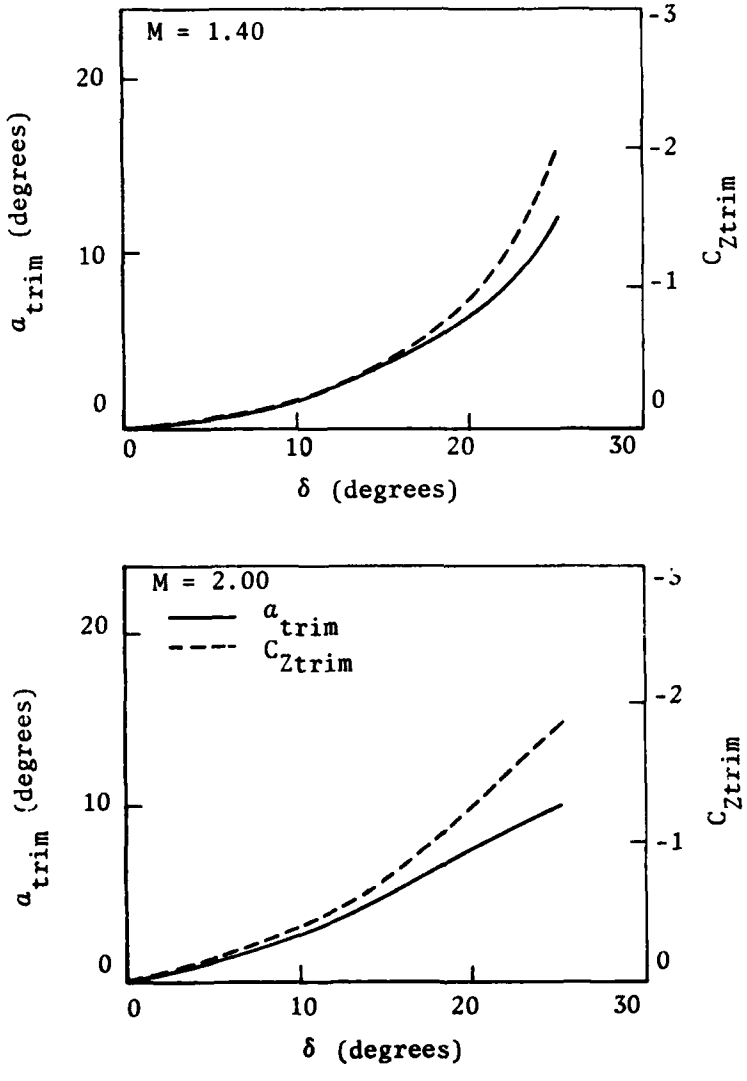

Figure 10(Contd.).

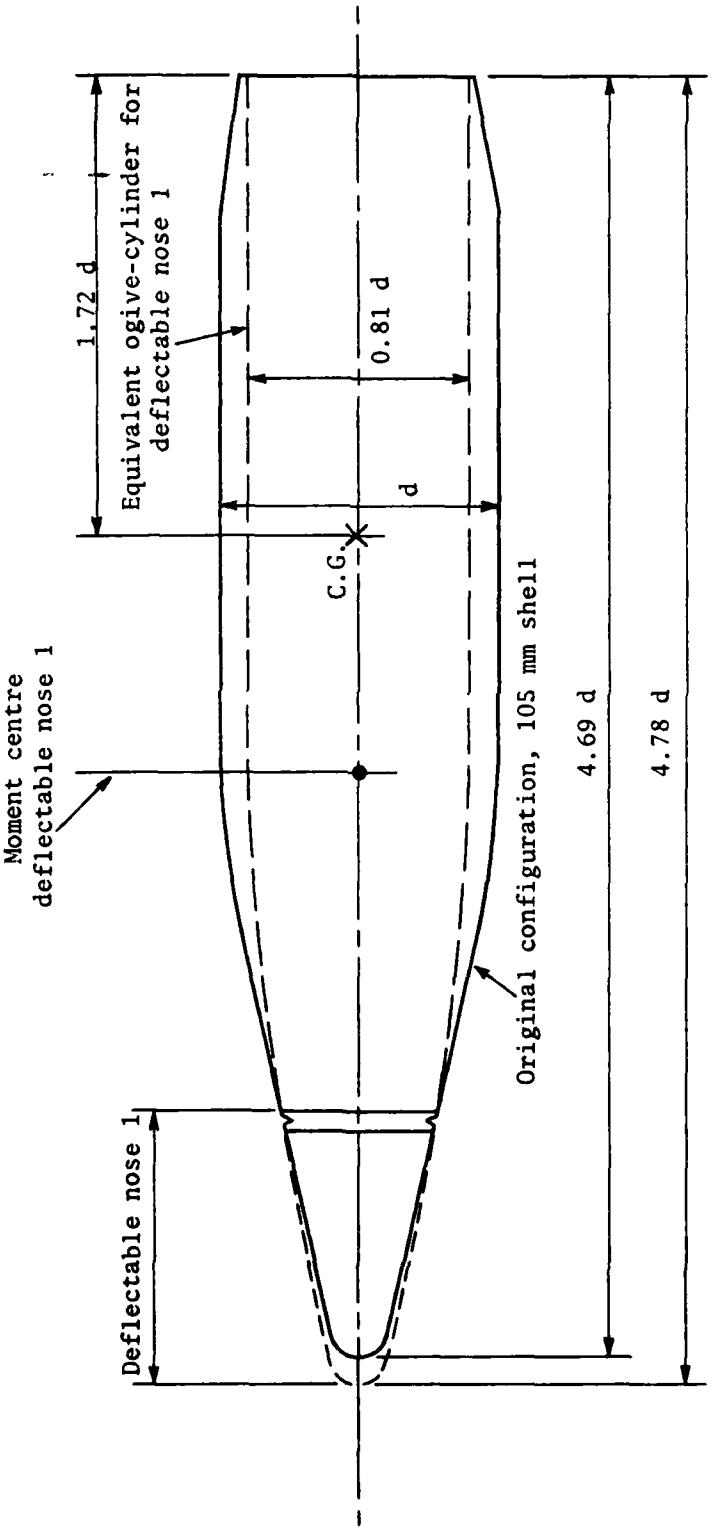

(a) Deflectable nose 1

Figure 11. 105 mm shell with two different deflectable noses

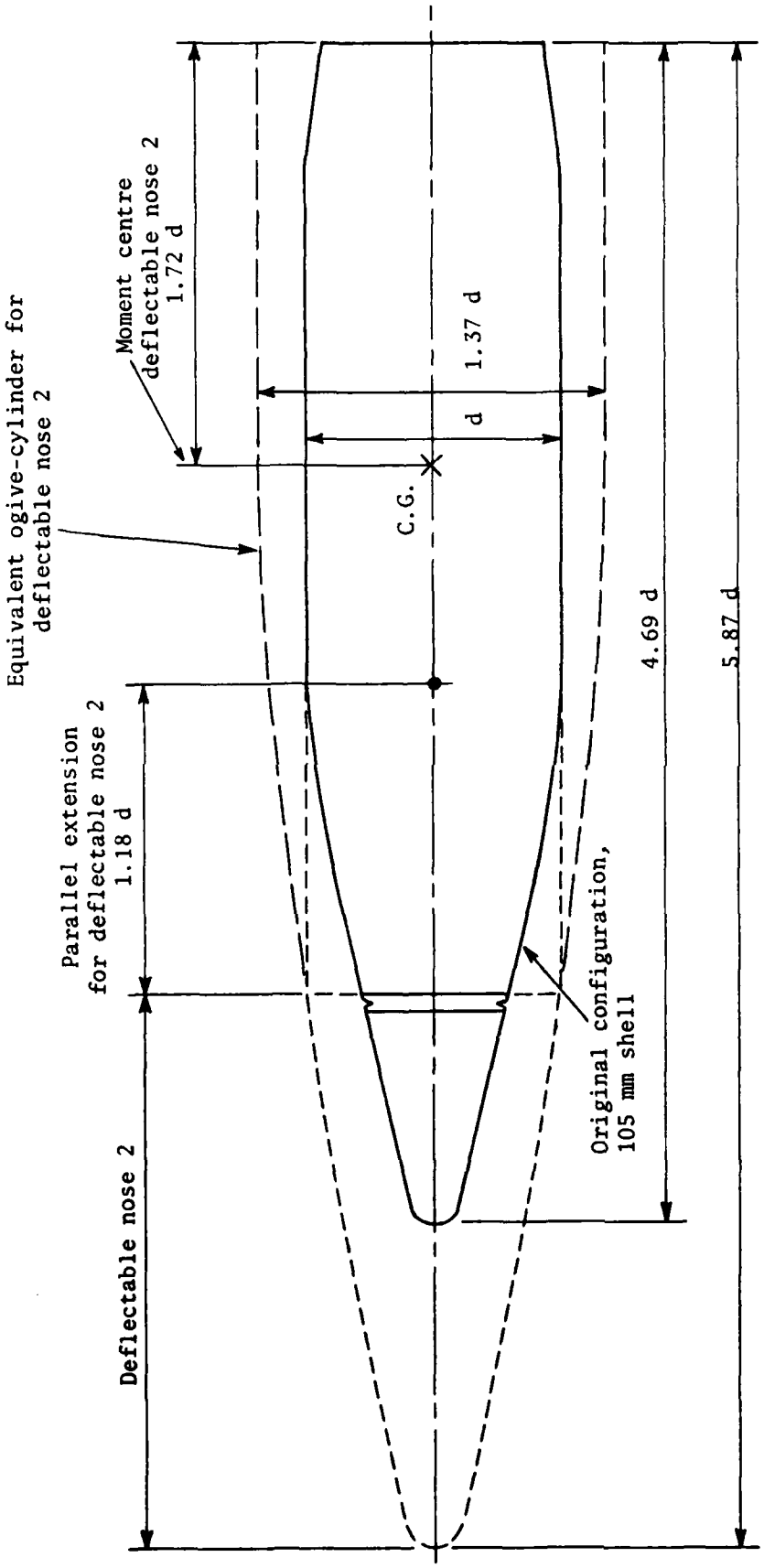

(b) Deflectable nose 2

Figure 11(Contd.).

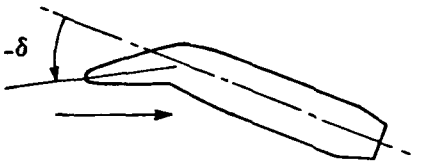

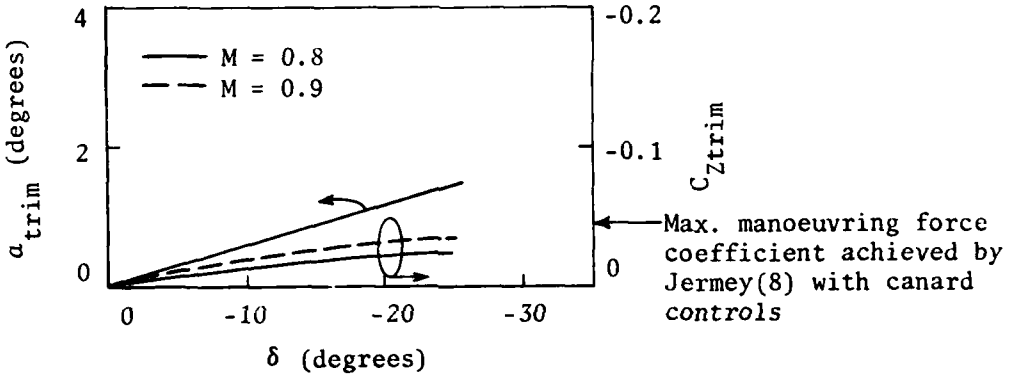

(a) Deflectable nose 1

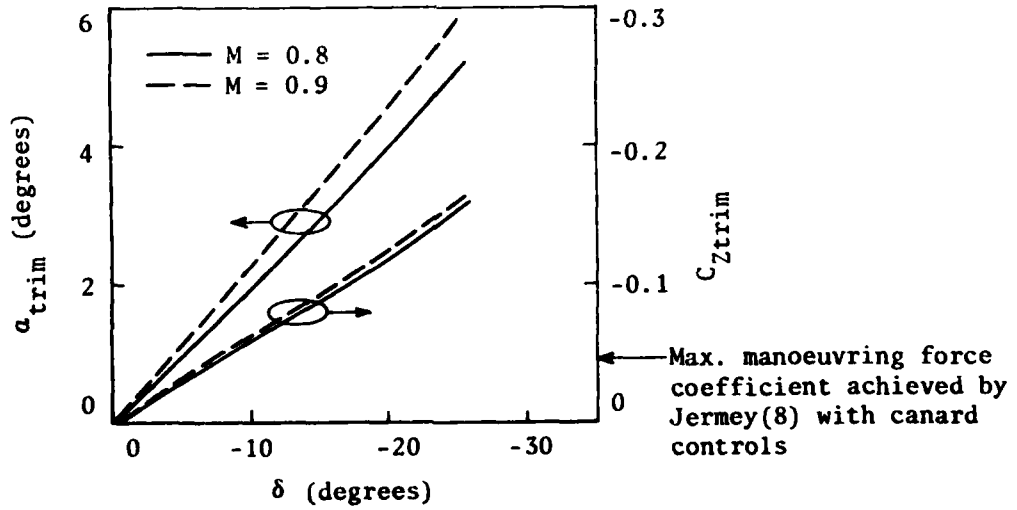

(b) Deflectable nose 2

Figure 12. Trim curves for 105 mm shell with two different deflectable noses

DISTRIBUTION

	Copy No.
EXTERNAL	
In United Kingdom	
Defence Scientific & Technical Representative, London	No copy
British Library Lending Division, Boston Spa, Yorkshire	1
UK National Leader, TTCP TP W-2	2 - 5
Technology Reports Centre, Orpington, Kent	6
In United States of America	
Counsellor, Defence Science, Washington	No copy
US National Leader, TTCP TP W-2	7 - 10
National Technical Information Services	11
Engineering Societies Library, New York	12
NASA Scientific & Technical Information Office, Washington DC	13
In Canada	
Canadian National Leader, TTCP TP W-2	14 - 17
In Australia	
Chief Defence Scientist	18
Deputy Chief Defence Scientist	19
Director, Joint Intelligence Organisation (DDSTI)	20
Superintendent, Science & Technology Programmes	21
Navy Scientific Adviser	22
Army Scientific Adviser	23
Air Force Scientific Adviser	24
Document Exchange Centre Defence Information Services Branch (for microfilming)	25
Defence Information Services Branch for:-	
United Kingdom, Ministry of Defence, Defence Research Information Centre (DRIC)	26
United States, Defense Technical Information Center	27 - 38
Canada, Department of National Defence, Defence Science Information Service	39
New Zealand, Ministry of Defence	40
Australian National Library	41
Director General, Army Development (NCO), Russell Offices For ABCA Standardisation Officers	
US ABCA representative, Canberra	42
UK ABCA representative, Canberra	43
Canada ABCA representative, Canberra	44
New Zealand ABCA representative, Canberra	45

	Copy No.
Director, Industry Development, Regional Office, Adelaide	46
Superintendent, RAN Research Laboratory	47
Head, Engineering Development Establishment	48
Defence Library, Campbell Park	49
Library, Aeronautical Research Laboratories	50
Library, Materials Research Laboratories	51

WITHIN DRCS

Chief Superintendent, Weapons Systems Research Laboratory	52
Superintendent, Aeroballistics Division	53
Superintendent, Propulsion Division	54
Superintendent, Weapon Systems Division	55
Principal Engineer, Air Weapons Engineering	56
Senior Principal Research Scientist, Ballistics	57
Principal Officer, Aerodynamic Research Group	58
Principal Officer, Dynamics Group	59
Principal Officer, Flight Research Group	60
Principal Officer, Ballistic Studies Group	61
Principal Officer, Field Experiments Group	62
Author	63
DRCS Library	64 - 65
AD Library	66 - 67
Spares	68 - 73

DOCUMENT CONTROL DATA SHEET

Security classification of this page: UNCLASSIFIED

1 DOCUMENT NUMBERS	
AR Number:	AR-002-583
Report Number:	WSRL-0211-TR
Other Numbers:	

2 SECURITY CLASSIFICATION	
a. Complete Document:	Unclassified
b. Title in Isolation:	Unclassified
c. Summary in Isolation:	Unclassified

3 TITLE

THE USE OF A DEFLECTABLE NOSE ON A MISSILE AS A CONTROL DEVICE

4 PERSONAL AUTHOR(S):

K.D. Thomson

5 DOCUMENT DATE:

May 1981

6 6.1 TOTAL NUMBER OF PAGES: 60

6.2 NUMBER OF REFERENCES: 8

7 7.1 CORPORATE AUTHOR(S):

Weapons Systems Research Laboratory

7.2 DOCUMENT SERIES AND NUMBER

Weapons Systems Research Laboratory 0211-TR

8 REFERENCE NUMBERS

a. Task:	DST 76/118
b. Sponsoring Agency:	DSTO

9 COST CODE:

10 IMPRINT (Publishing organisation)

Defence Research Centre Salisbury

11 COMPUTER PROGRAM(S) (Title(s) and language(s))

12 RELEASE LIMITATIONS (of the document):

Approved for Public Release

12.0	OVERSEAS	NO		P.R.	1	A		B		C		D		E	

Security classification of this page: UNCLASSIFIED

Security classification of this page: UNCLASSIFIED

13 ANNOUNCEMENT LIMITATIONS (of the information on these pages):

No limitation

14 DESCRIPTORS:

a. EJC Thesaurus Terms

Missile guidance
Impact prediction
Projectiles
Missiles
Control equipment
Wind tunnel tests
Nose cones
Mach number
Deflection

b. Non-Thesaurus Terms

Deflectable noses

15 COSATI CODES

1604

16 LIBRARY LOCATION CODES (for libraries listed in the distribution):

17 SUMMARY OR ABSTRACT:
(if this is security classified, the announcement of this report will be similarly classified)

Wind tunnel tests have been carried out on a blunted ogive-cylinder with a deflectable nose at Mach numbers between 0.8 and 2.0. Although the results are subject to scale effects, it appears that the deflectable nose could find use as a missile control method.

The results have been applied to two missile configurations. For a long slender missile the deflectable nose produces non-linear trim curves at subsonic speeds, approaching linearity at supersonic Mach numbers. Nevertheless, worthwhile trimmed incidences can be achieved. Although a deflectable nose on a 105 mm shell at subsonic speeds produces only relatively small normal force coefficients at trim, the trim curves are linear. Furthermore, it appears that when used for terminal control significant deviations in shell impact point are attainable.

Security classification of this page: UNCLASSIFIED

The official documents produced by the Laboratories of the Defence Research Centre Salisbury are issued in one of five categories: Reports, Technical Reports, Technical Memoranda, Manuals and Specifications. The purpose of the latter two categories is self-evident, with the other three categories being used for the following purposes:

Reports	:	documents prepared for managerial purposes.
Technical Reports	:	records of scientific and technical work of a permanent value intended for other scientists and technologists working in the field.
Technical Memoranda	:	intended primarily for disseminating information within the DSTO. They are usually tentative in nature and reflect the personal views of the author.